

Original Articles

Predicting the likelihood of a desirable ecological regime shift: A case study in Cootes Paradise marsh, Lake Ontario, Ontario, Canada

Cindy Yang^a, Dong-Kyun Kim^a, Jennifer Bowman^b, Tys Theësmeyer^b, George B. Arhonditsis^{a,*}^a Ecological Modelling Laboratory, Department of Physical & Environmental Sciences, University of Toronto, Toronto, Ontario M1C 1A4, Canada^b Royal Botanical Gardens, Burlington, Ontario L7T 4H4, Canada

ARTICLE INFO

Keywords:

Wetland restoration
Phosphorus
Regime shift
Macrophytes
Mechanistic model
Bayesian inference

ABSTRACT

Environmental modelling is one of the pillars of the management process, representing an “information integrator” that brings together scientists, managers, and other stakeholders in a joint assessment of our understanding of the system being managed and the compelling knowledge gaps we seek to answer through monitoring and research. The overarching goal of the present modelling study is to offer insights into the restoration and management of Cootes Paradise marsh, one of the most degraded shallow wetlands in Southern Ontario. We use a mechanistic model to leverage our understanding of the major phosphorus biogeochemical pathways in Cootes Paradise. We also develop a network of statistical models that accommodates the spatial heterogeneity of the prevailing water quality conditions in the marsh. Combining the insights from both models, we found that a drastic reduction of point- and nonpoint-source nutrient loading could trigger a non-linear shift from the current turbid-phytoplankton dominated state to a clear-macrophyte dominated state. The restoration trajectory of the system can be profoundly modulated by the presence of a thriving macrophyte community with an enhanced ability to sequester phosphorus (i.e., the net amount of phosphorus taken up per unit of plant tissue). Critical remedial actions to re-establish the targeted macrophyte species in their native marsh habitats include both the intensification of local planting efforts and the control of invasive plant species. Another important finding of our modelling analysis is that the signature of the water quality improvements brought about by nutrient loading reductions dissipates as we move from the marsh’s western end to the central area due the presence of confounding factors, such as the hydraulic loading from Spencer Creek, internal nutrient loading, wind resuspension, and bioturbation. Given the high uncertainties associated with forecasting drastic (and costly) remedial actions, we argue in favour of a socioeconomic assessment of Cootes Paradise marsh as an ecosystem service provider to determine the benefits in terms of monetary values when we examine different courses of management options.

1. Introduction

Coastal wetlands are among the world’s most productive ecosystems and provide a wide range of ecosystem services with considerable benefits for human societies (Barbier et al., 1997). Wetlands host rich biodiversity, represent an important spawning/nursery habitat and shelter for commercial fish, and protect shorelines from erosion events (Millennium Ecosystem Assessment, 2005). The loss of coastal wetlands is a topical issue in environmental sciences, especially in the Great Lakes region, where 60–80% of coastal wetlands have already been lost since the 1800s (Smith et al., 2001; Government of Canada, 2016). The degradation of these ecologically and economically significant ecosystems stems from land-use conversion, shoreline development, cultural eutrophication, water level fluctuations, and bioturbation by invasive

species (Croft and Chow-Fraser, 2007; Janse et al., 2019; Kim et al., 2016; Lougheed and Chow-Fraser, 1998). Consequently, cooperative binational programs, such as the Great Lakes Water Quality Agreement (GLWQA), have been developed with the mandate to create, reclaim, rehabilitate, and protect wetland habitats in the Great Lakes basin (Government of Canada, 2017). The GLWQA calls for localized, concentrated efforts to restore degraded locations through the development of clean-up plans that identify restoration actions necessary for the recovery of wetland ecosystems.

A characteristic example of a degraded rivermouth wetland is Cootes Paradise marsh, which is located on the west side of Hamilton Harbour at the western end of Lake Ontario (Fig. 1). Owing to its size and location, the marsh is contained within a nature reserve and serves as an important migratory waterfowl staging habitat, one of the largest

* Corresponding author.

E-mail address: georgea@utsc.utoronto.ca (G.B. Arhonditsis).

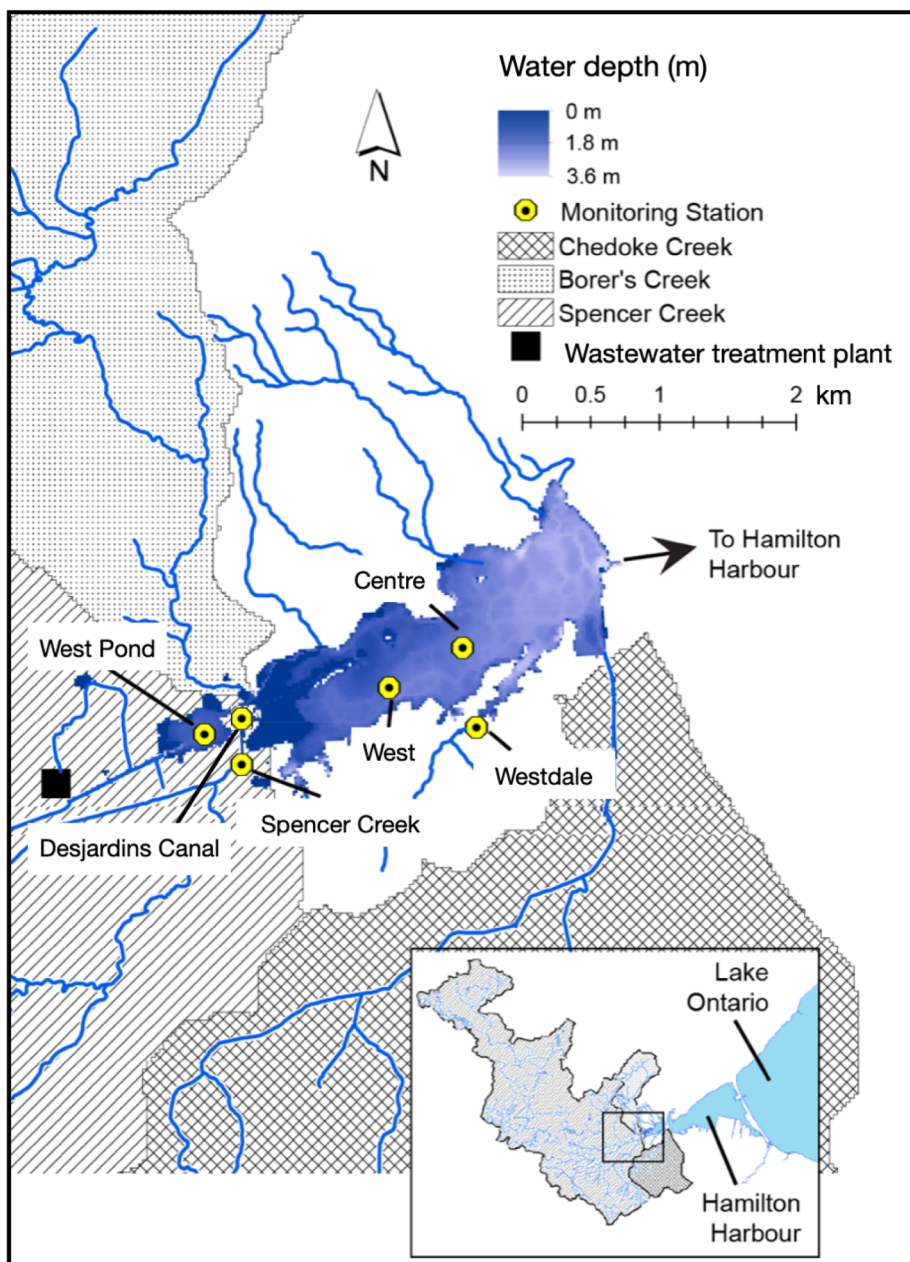


Fig. 1. Cootes Paradise marsh draining into the western end of Hamilton Harbour in Lake Ontario.

fish nursery habitats in Southern Ontario, as well as an area of socio-economic interest with valuable ecosystem services, such as water filtration, shoreline and storm protection, and support of tourism and recreational activities (Thomasen and Chow-Fraser, 2012). Because of the multitude of anthropogenic activities hosted in the surrounding watershed, Cootes Paradise marsh has shifted from a clear macrophyte-dominated state to a turbid phytoplankton-dominated state since the 1930s (Chow-Fraser et al., 1998). Submergent macrophyte loss has been attributed to reduced water clarity from wind-driven sediment resuspension and the invasive common carp (*Cyprinus carpio*); excess nutrient inflows from agricultural, residential, industrial, and commercial sources; sewage effluent discharged from the Dundas Wastewater Treatment Plant (WWTP); and combined sewer overflows (CSOs) from the City of Hamilton, which have collectively triggered water quality degradation and fish habitat disruption (Thomasen and Chow-Fraser, 2012). The ramifications for Cootes Paradise marsh have been the loss of abundance and diversity in the macrophyte community, as well as the decline in native fish and wildlife populations (Smith et al.,

2001; Lougheed et al., 2004; Kim et al., 2016). In its current turbid and degraded state, the waters flowing through the marsh represent a major polluting contributor to Hamilton Harbour, accounting for >20% of total phosphorus (TP) variability (Gudimov et al., 2011), which further reinforces the urgency for its restoration.

Several initiatives have been implemented to restore Cootes Paradise marsh, including the improved capture and treatment of four combined sewer overflows (1994–2012), a stewardship program in the agricultural portion of the watershed (beginning in 1994), a plant species re-introduction program (beginning in 1994), and the construction of a fishway barrier (see Fig. 1) at the marsh's outlet in 1997 to mechanistically exclude large common carp (>40 cm) and promote the recovery of native fish populations (Theysmeijer, 2011; Theysmeijer et al., 2016). Given that carp activity can indirectly favour algal growth since they uproot submerged macrophytes and perturb the sediments, Lougheed and Chow-Fraser (1998) predicted that the exclusion of common carp could be responsible for anywhere between 25–45% reduction in turbidity. Likewise, Chow-Fraser (2005) predicted a 25%

decrease of total suspended solids after parsing out the effects of inter-annual variability in water levels, which in turn could –in principle– mediate a shift of the marsh to a clear macrophyte-dominated state (Moss et al., 1996; Madgwick, 1999; Ibelings et al., 2007; Thomasen and Chow-Fraser, 2012; Leisti et al., 2016). As previously mentioned, a barrier (or fishway) was constructed to restore aquatic vegetation in Cootes Paradise marsh, and successfully reduced carp biomass from an estimated average marsh-wide biomass of 80 to 5 tonnes km⁻² (Wilcox and Whillans, 1999; Lougheed et al., 2004). Although conditions have improved immensely in the sheltered inlets, the main flow through the marsh remains hypereutrophic. The light environment, for the sediment surface of the deep, open-water sites, remains prohibitive to reliably support the growth of submerged aquatic vegetation. Consequently, the plants sustained have primarily been mats of filamentous algae that limit the growth of desirable submergent vegetation (Theysmeijer and Bowman, 2017). Phytoplankton growth peaks in August when tributary flows typically reach their seasonal minima, making the steady and relatively high TP inflows from Dundas WWTP the dominant exogenous nutrient source.

Notwithstanding the recent water quality improvements, the marsh has not transitioned back to its former clear macrophyte-dominated state as of yet. Likewise, fish and wildlife populations have not responded to the relatively improved marsh conditions, and only the fish abundance of low oxygen tolerant species has increased. The persistence of the turbid phytoplankton-dominated state may be partially attributed to the presence of feedback biogeochemical mechanisms (Scheffer et al., 2001; Suding et al., 2004), and therefore the desired shift to a clear macrophyte-dominated state may not be realized in the foreseeable future without additional remedial measures (Thomasen and Chow-Fraser, 2012; Kim et al., 2016). In this regard, the City of Hamilton with contributions from the federal and provincial governments, has undertaken initiatives to improve water quality by reducing point-source loading from Dundas WWTP into Cootes Paradise marsh. In 2013, the City completed \$2.4 million worth of upgrades to Dundas WWTP to provide additional environmental protection (Infrastructure Canada, 2013). As the plant is over 30 years old, City staff are pursuing even greater water quality improvements as part of its renewal and evaluating additional upgrades to improve effluent treatment performance, with options ranging from \$20.4 million to more than \$35 million (<https://www.hamiltonnews.com/news-story/7007821-dundas-wastewater-treatment-plant-needs-upgrades-to-meet-targets/>), towards achieving an average TP target of 50 µg L⁻¹ and an average chlorophyll α (hereafter Chla) concentration of 20 µg L⁻¹ (Kim et al., 2016). The questions arising though are whether the planned restorative actions are capable of inducing such a desirable ecological regime shift in Cootes Paradise marsh, or if the new clearer state will be resilient to the influence of other internal mechanisms (sediment diagenesis, nutrient recycling, wind resuspension) and external stressors (e.g., urbanization, agricultural activities).

To this end, the present study introduces a network of data-driven and process-based models for Cootes Paradise marsh, which are used to estimate the critical nutrient loads that will bring the system closer to the existing water quality goals (i.e., Chla and TP targets). Our mechanistic model is used to elucidate the interplay among different biogeochemical mechanisms (resource-competition processes within the autotrophic assemblage, sediment diagenesis, P sequestration from macrophytes) that drive the local water quality conditions in Cootes Paradise. We also develop a feedforward system of regression models that link the eutrophic conditions in the innermost western segment with the western and, ultimately, the central area of the main marsh. Our modelling analysis offers a synthesis of our best ecological understanding of wetland dynamics in Cootes Paradise marsh and predicts the ecosystem response to a combination of point-source loading reductions and degrees of re-establishment of the submerged macrophyte community. By leveraging the complementary strengths of data-driven and process-based models, this multi-model approach provides a more

comprehensive and robust characterization of Cootes Paradise's state and the actions needed for its recovery. Viewing ecosystems as providers of economically valuable benefits to humans, our study concludes by advocating for the development of a rigorous framework that quantifies the importance of a well-functioning ecosystem in monetary terms. Our thesis is that this could be a critically important strategy to gain leeway and support investments to the restoration of Cootes Paradise, even if the multitude of abiotic and biotic factors that shape its dynamics introduce considerable uncertainty into the decision-making process.

2. Methods

2.1. Study site-Dataset description

Cootes Paradise marsh is a shallow, hypereutrophic rivermouth wetland that is hydraulically connected to Hamilton Harbour by a man-made channel, known as the Desjardins Canal (Fig. 1). It is the largest remaining coastal marsh in Lake Ontario with three main tributaries draining the surrounding watershed: Spencer, Chedoke, and Borer's Creeks. The marsh is approximately 4-km long and 1-km wide with a mean depth of 0.7 m. The surface area and volume can vary significantly according to the water level fluctuations, reaching a maximum of 2.5 km² and 3.6 × 10⁶ m³, respectively (Mayer et al., 2005; Leisti et al., 2016). Cootes Paradise marsh is designated, as part of the Royal Botanical Gardens Nature Reserve properties and the Niagara Escarpment World Biosphere Reserve, an Area of Natural and Scientific Interest and a Class 1 provincially significant wetland (Theysmeijer, 2011). The marsh is an important migratory location for waterfowl, as well as a major fish nursery. However, for the past nine decades, Cootes Paradise marsh has transitioned from having 90% areal coverage of diverse submergent and emergent vegetation to less than 15% (Chow-Fraser et al., 1998). Submergent vegetation loss has been attributed to reduced water clarity associated with sediment resuspension from wind and invasive common carp (*Cyprinus carpio*) activity, as well as excessive nutrient inputs from the runoff of adjacent agricultural, residential, industrial, commercial and recreational areas, sewage effluents discharged from Dundas WWTP, and CSOs from the City of Hamilton (Thomasen and Chow-Fraser, 2012). Emergent vegetation loss has been mainly attributed to the sustained high water levels in Lake Ontario over the past 30 years, as well as the physical destruction by carp (Lougheed et al., 2004).

The Royal Botanical Gardens provided bi-monthly water quality data for the three major tributaries (Spencer downstream, Chedoke, and Borer's Creeks), Westdale Creek, Cootes-West, and Cootes-Centre monitoring stations from May to September during the 1994–2016 period. Details on the sampling network and monitoring results can be found in Mataya et al. (2017). Of the three main tributaries draining into Cootes Paradise, daily discharge data for the entire historical period were available only for Spencer Creek and were obtained from the Water Survey of Canada (WSC) Dundas flow gauge station (Kim et al., 2016). A correction factor of 1.39 was subsequently used to adjust the areal ratio of drainage between the creek mouth and the Dundas monitoring site (Theysmeijer et al., 2009). Due to the lack of data for Chedoke and Borer's creeks, daily flow discharge was estimated by applying correction factors based on tributaries with available data and similar watershed characteristics. Specifically, we applied correction factors to discharge rates from Redhill and Grindstone Creeks to derive flow estimates for Chedoke and Borer's Creek, respectively (Theysmeijer et al., 2009; Kim et al., 2016). WWTP loading estimates were based on monthly flows and effluent TP concentrations from Dundas WWTP, as reported by the City of Hamilton. CSO loading estimates into Cootes Paradise were based on two data sources: the Wastewater Treatment Facilities Annual Report (HHWQTT, 2007) and the Contaminant Loading Report (HHRAPTT, 2010). CSO volume estimates were based on continuous field measurements in overflow tanks,

while a fixed concentration, based on the average measured *TP* concentrations from CSO tank influent, was used to calculate loading values (Kim et al., 2016). Further details for the determination of non-point- and point-source loading estimates are provided in the Supporting Information of Kim et al. (2016).

2.2. Modelling framework

2.2.1. Mechanistic modelling

We simulated eutrophication dynamics during the growing season (May–October) in Cootes Paradise marsh for a 17-year (1996–2012) period with the Wetland Eutrophication Model (*WEM*) (Kim et al., 2018). *WEM* comprises the following state variables: dissolved- and particulate-phase phosphorus in the water column, including phosphorus sequestered within the cells of three functional phytoplankton and macrophyte (meadow, emergent and submerged) groups, sediment-particulate phosphorus in labile, refractory, and inert forms, as well as dissolved phosphorus in interstitial waters (Fig. S1). The relative amount of each of the three *TP* fractions in the water column is modulated by a suite of biogeochemical processes: uptake by the primary producers, respiration/mortality of the biotic components, bacterial-mediated mineralization, sediment resuspension, organic matter decomposition, diffusion, and particle settling (Kim et al., 2018). Dissolved phosphorus in interstitial waters is lost through macrophyte uptake and sediment diffusive reflux, while sediment particulate phosphorus is removed through sediment resuspension and burial. Phosphorus in interstitial waters is also replenished through temperature-dependent decomposition.

WEM's phytoplankton module is based on Arhonditis and Brett's (2005) and Ramin et al.'s (2011) models by explicitly considering three phytoplankton functional groups with distinct ecophysiological characteristics. A diatom-like group represents an "r-strategist" with fast growth/metabolic rates, fast settling rates, and superior phosphorus kinetics, whereas a cyanobacteria-like group resembles a "K-strategist" that is characterized by slow settling rates and inferior phosphorus kinetics. We also considered a third group that was specified as an intermediate between diatoms and cyanobacteria. Similar to the phytoplankton governing equations, *WEM* simulates macrophyte growth as a function of nutrients, temperature and light availability, but there are four key differences between macrophyte and phytoplankton processes with respect to resource (light and nutrient) procurement: (i) photosynthesis rates by submerged macrophytes are strongly impacted by light attenuation and exhibit an inverse relationship with water depth, whereas meadow and emergent plants do not experience light limitation (Kim et al., 2018); (ii) meadows and emergent macrophytes exert light-shading effects on submerged macrophyte and phytoplankton growth (Kim et al., 2018); (iii) macrophytes uptake phosphorus from both water column and interstitial waters with an uptake ratio that varies according to the relative phosphorus abundance of the two pools (Granéli and Solander, 1988; Christiansen et al., 2016); and (iv) phosphorus retention in macrophyte tissues assumes that half of the taken phosphorus is recycled through slow decomposition of dead plant tissues, while the other half is rapidly released through respiration (Asaeda et al., 2000). *WEM*'s differential equations, parameter definitions, and other assumptions are presented in Kim et al. (2018).

2.2.2. Statistical modelling

In the absence of hydrodynamic data, a major *WEM* assumption is that the Cootes Paradise marsh is a homogeneous (completely mixed) system without any discernible gradients characterizing its water quality patterns. Given the marsh's small size (Fig. 1), this assumption is presumably defensible (especially on a seasonal scale), but historical data provided by the Royal Botanical Gardens (RBG) show a tendency for a westward *TP* gradient, i.e., $160 \pm 81 \mu\text{g TP L}^{-1}$ at the Cootes-Centre station versus $202 \pm 119 \mu\text{g TP L}^{-1}$ at West-Pond, during the growing season between 1994 and 2013, whereas an eastward (but weaker) gradient held true with respect to the Chla concentrations, i.e.,

Cootes-Centre ($42 \pm 33 \mu\text{g L}^{-1}$) versus Cootes-West ($37 \pm 28 \mu\text{g L}^{-1}$). Interestingly, the Chla concentrations at the innermost western segment displayed significant variability with values varying from 6 to $457 \mu\text{g Chla L}^{-1}$, reflecting watershed flows along with the influence of urban runoff events. To emulate these water quality patterns over the course of a 20-yr (1994–2013) period, we developed a feedforward system of cause-effect relationships in three segments of Cootes Paradise (West-Pond, Cootes-West, Cootes-Centre), whereby the ambient *TP* level in each segment is used as a predictor for its counterpart in the succeeding segment. In addition, a fourth model was developed to connect *TP* with Chla concentrations in Cootes-Centre, the central area of Cootes Paradise marsh (Fig. 2). To the best of our knowledge, this is the first attempt to accommodate the spatial heterogeneity in Cootes Paradise since the mechanistic model presented by Prescott and Tsanis (1997).

We used Bayesian inference to estimate model parameters because of its ability to quantify model structural/parametric uncertainty as well as to accommodate the uncertainty pertaining to missing data and measurement errors (Gelman et al., 2013). Bayesian inference treats each parameter θ as a random variable and uses the likelihood function to express the relative plausibility of different parameter values given the available data from the system:

$$P(\theta|data) = \frac{P(\theta)P(data|\theta)}{\int_{\theta} P(\theta)P(data|\theta)d\theta}$$

where $P(\theta)$ represents the prior distribution of the model parameter θ , $P(data|\theta)$ indicates the likelihood of the data observation given the different θ values, and $P(\theta|data)$ is the posterior probability representing our updated beliefs on the θ values, contingent upon empirical knowledge from the system. The denominator is often referred to as the marginal distribution of the available data and acts as a scaling constant that normalizes the integral of the area under the posterior probability distribution (Gelman et al., 2013).

The first model of our feedforward system aims to describe the ambient *TP* levels in the innermost western segment of Cootes Paradise marsh, West-Pond, using the *TP* concentrations and associated flows of the treated sewage discharged from Dundas WWTP as explanatory variables. The mathematical formulation of the first model is summarized as follows:

$$\begin{aligned} \ln[\widehat{TP}_{ijt}]_{WP} &= \beta_{WP0} + \beta_{WP1}\ln[TP_{ijt}]_{Dundas} + \beta_{WP2}\ln[Q_{ijt}]_{Dundas} \\ \ln[TP_{ijt}]_{WP} &\sim N(\ln[\widehat{TP}_{ijt}]_{WP}, \sigma_{WP}^2) \\ \beta_{WPk} &\sim N(0, 10000); k = 0, 1, 2 \\ \sigma_{WP}^{-2} &\sim G(0.001, 0.001) \end{aligned}$$

where $\ln[TP_{ijt}]_{WP}$ and $\ln[\widehat{TP}_{ijt}]_{WP}$ are the natural logarithms of the measured and predicted *TP* concentrations ($\ln[\mu\text{g TP L}^{-1}]_{WP}$) of sample i that is collected from West-Pond in month j and year t ; β_{WP0} refers to the baseline intercept of the model ($\ln[\mu\text{g TP L}^{-1}]_{WP}$); $\ln[TP_{ijt}]_{Dundas}$ represents the natural logarithm of the measured *TP* concentrations ($\ln[\mu\text{g TP L}^{-1}]_{Dundas}$) in the effluents from Dundas WWTP; β_{WP1} is the regression coefficient reflecting the relationship between *TP* concentrations of the treated sewage and those at West-Pond ($\ln[\mu\text{g TP L}^{-1}]_{WP}/\ln[\mu\text{g TP L}^{-1}]_{Dundas}$)^{1*}; $\ln[Q_{ijt}]_{Dundas}$ is the natural logarithm of the measured flow ($\ln[m^3 s^{-1}]_{Dundas}$) from Dundas WWTP; β_{WP2} is the corresponding regression coefficient ($\ln[\mu\text{g TP L}^{-1}]_{WP}/\ln[m^3 s^{-1}]_{Dundas}$); σ_{WP} refers to the structural error of the model; $N(0, 10000)$ is the normal distribution with mean 0 and variance 10000; and $G(0.001, 0.001)$ is the gamma distribution with shape and scale parameters of 0.001. These prior distributions are considered "non-informative".

The second model of our feedforward system links the *TP*

¹ Parameters with asterisk are unitless. The selected presentation of their units is intended to facilitate their interpretation.

concentrations in the western area of the main marsh, Cootes-West, with the TP concentrations at West-Pond (the preceding segment), and the riverine TP and hydraulic loading from Spencer Creek. The mathematical formulation of the second model is summarized as follows:

$$\ln[\widehat{TP}_{ijt}]_{CW} = \beta_{CW0} + \beta_{CW1}\ln[TP_{ijt}]_{WP} + \beta_{CW2}\ln[TP_{ijt}]_{SC} + \beta_{CW3}\ln[Q_{ijt}]_{SC}$$

$$\ln[TP_{ijt}]_{CW} \sim N(\ln[\widehat{TP}_{ijt}]_{CW}, \sigma_{CW}^2)$$

$$\beta_{CWk} \sim N(0, 10000); k = 0, 1, 2, 3$$

$$\sigma_{CW}^{-2} \sim G(0.001, 0.001)$$

where $\ln[TP_{ijt}]_{CW}$ and $\ln[\widehat{TP}_{ijt}]_{CW}$ are the natural logarithms of the measured and predicted TP concentrations ($\ln[\mu\text{g TP L}^{-1}]_{CW}$) of sample i collected from Cootes-West in month j and year t ; β_{CW0} is the intercept of the model ($\ln[\mu\text{g TP L}^{-1}]_{CW}$); $\ln[TP_{ijt}]_{WP}$ represents the natural logarithm of the TP concentrations ($\ln[\mu\text{g TP L}^{-1}]_{West-Pond}$) at West-Pond; β_{CW1} is the associated regression coefficient ($\ln[\mu\text{g TP L}^{-1}]_{CW}/\ln[\mu\text{g TP L}^{-1}]_{WP}$)*; $\ln[TP_{ijt}]_{SC}$ and $\ln[Q_{ijt}]_{SC}$ are the natural logarithms of the TP concentrations ($\ln[\mu\text{g TP L}^{-1}]_{SC}$) and flows ($\ln[m^3 s^{-1}]_{SC}$) registered at Spencer Creek; β_{CW2} ($\ln[\mu\text{g TP L}^{-1}]_{CW}/\ln[\mu\text{g TP L}^{-1}]_{SC}$)* and β_{CW3} ($\ln[\mu\text{g TP L}^{-1}]_{CW}/\ln[m^3 s^{-1}]_{SC}$) are the corresponding regression coefficients; and σ_{CW} denotes the structural error of the model.

The third model describes the TP concentrations in the central marsh, Cootes-Centre, as a function of the ambient TP levels at Cootes-West (the preceding segment), while accommodating the within- and among-year TP variability in the central area.

$$\ln[\widehat{TP}_{ijt}]_{CC} = \beta_{CC0} + \beta_{CC1}\ln[TP_{ijt}]_{CW} + \beta_{CCYt} + \beta_{CCMj}$$

$$\ln[TP_{ijt}]_{CC} \sim N(\ln[\widehat{TP}_{ijt}]_{CC}, \sigma_{CC}^2)$$

$$\beta_{CCk} \sim N(0, 10000); k = 0, 1$$

$$\beta_{CCYt} \sim N(\mu_{CCY}, \sigma_{CCY}^2); \sum_{t=1}^T \beta_{CCYt} = 0$$

$$\beta_{CCMj} \sim N(\mu_{CCM}, \sigma_{CCM}^2); \sum_{j=1}^J \beta_{CCMj} = 0$$

$$\mu_{CCY} \sim N(0, 10000); \mu_{CCM} \sim N(0, 10000)$$

$$\sigma_{CCY}^{-2} \sim G(0.001, 0.001); \sigma_{CCM}^{-2} \sim G(0.001, 0.001)$$

$$\sigma_{CC}^{-2} \sim G(0.001, 0.001)$$

where $\ln[TP_{ijt}]_{CC}$ and $\ln[\widehat{TP}_{ijt}]_{CC}$ are the natural logarithms of the measured and predicted TP concentrations ($\ln[\mu\text{g TP L}^{-1}]_{CC}$) of sample i collected from Cootes-Centre in month j and year t ; β_{CC0} is the intercept of the model ($\ln[\mu\text{g TP L}^{-1}]_{CC}$); $\ln[TP_{ijt}]_{CC}$ represents the natural logarithm of the TP concentrations ($\ln[\mu\text{g TP L}^{-1}]_{CC}$) at Cootes-West; β_{CC1} is the associated regression coefficient ($\ln[\mu\text{g TP L}^{-1}]_{CC}/\ln[\mu\text{g TP L}^{-1}]_{CW}$)*; σ_{CC} represents the structural error of the model; β_{CCYt} and β_{CCMj} are the among- and within-year effect terms. The latter parameters are specified by a hierarchical formulation, whereby among- and within-year effects are drawn from two global distributions that are specified by mean values of and μ_{CCM} and variances of σ_{CCY}^2 and σ_{CCM}^2 , respectively; T and J are the total number of years t (=20) and the number of months j (=5) of the growing season, respectively. To facilitate parameter identification, we constrained the within- and among-year effect terms to have a zero sum.

The fourth model connects the Chla concentrations in the central marsh, Cootes-Centre, with the ambient TP levels at the same segment (predicted by the third model), as well as those registered at the Westdale inlet. The Westdale inlet is a sheltered site located along the south side of Cootes Paradise marsh, and receives water from Westdale Creek. Westdale Creek is a spring-fed creek with a sewer-overflow location at its headwater (Reddick and Theysmeyer, 2012). The model also explicitly considers the within- and among-year Chla variability in the central-outer segment of Cootes Paradise.

$$\ln[\widehat{Chla}_{ijt}]_{CC} = \gamma_{CC0} + \gamma_{CC1}\ln[TP_{ijt}]_{CC} + \gamma_{CC2}\ln[TP_{ijt}]_{WD} + \gamma_{CCYt} + \gamma_{CCMj}$$

$$\ln[Chla_{ijt}]_{CC} \sim N(\ln[\widehat{Chla}_{ijt}]_{CC}, \tau_{CC}^2)$$

$$\gamma_{CCk} \sim N(0, 10000); k = 0, 1, 2$$

$$\gamma_{CCYt} \sim N(\nu_{CCY}, \tau_{CCY}^2); \sum_{t=1}^T \gamma_{CCYt} = 0$$

$$\gamma_{CCMj} \sim N(\nu_{CCM}, \tau_{CCM}^2); \sum_{j=1}^J \gamma_{CCMj} = 0$$

$$\nu_{CCY} \sim N(0, 10000); \nu_{CCM} \sim N(0, 10000)$$

$$\tau_{CCY}^{-2} \sim G(0.001, 0.001); \tau_{CCM}^{-2} \sim G(0.001, 0.001)$$

$$\tau_{CC}^{-2} \sim G(0.001, 0.001)$$

where $\ln[Chla_{ijt}]_{CC}$ and $\ln[\widehat{Chla}_{ijt}]_{CC}$ are the natural logarithms of the measured and predicted Chla concentrations ($\ln[\mu\text{g Chla L}^{-1}]_{CC}$) of sample i from Cootes-Centre collected in month j and year t ; γ_{CC0} is the intercept of the model ($\ln[\mu\text{g Chla L}^{-1}]_{CC}$); $\ln[TP_{ijt}]_{CC}$ represents the natural logarithm of the TP concentrations ($\ln[\mu\text{g TP L}^{-1}]_{CC}$) at Cootes-Centre and γ_{CC1} is the associated regression coefficient ($\ln[\mu\text{g Chla L}^{-1}]_{CC}/\ln[\mu\text{g TP L}^{-1}]_{CC}$); $\ln[TP_{ijt}]_{WD}$ represents the natural logarithm of the TP concentrations ($\ln[\mu\text{g TP L}^{-1}]_{WD}$) at the Westdale inlet; γ_{CC2} is the associated regression coefficient ($\ln[\mu\text{g Chla L}^{-1}]_{CC}/\ln[\mu\text{g TP L}^{-1}]_{Westdale}$); γ_{CCYt} is the among-year effect term; γ_{CCMj} is the within-year effect term; ν_{CCY} and ν_{CCM} are the respective means of the hyperparameters of the site- and among-year effect terms; τ_{CCY}^2 and τ_{CCM}^2 are the respective variances of the hyperparameters; and τ_{CC} refers to the structural error of the model.

Statistical model computations: Sequences of realizations from the model posterior distributions were achieved by using Markov Chain Monte Carlo (MCMC) simulations (Gilks et al., 1998). We used a general normal proposal Metropolis algorithm, which is based on a symmetric normal proposal distribution whose standard deviation is adjusted over the first 4,000 iterations such that the acceptance rate ranges between 20% and 40%. For each analysis, we used three chain runs of 50,000 iterations, keeping every 20th iteration (thin of 20) to avoid serial correlation. We discarded the first 10,000 samples to eliminate the influence of the initial parameter values assigned (*burn-in*) and took samples after the MCMC simulation converged to the true posterior distribution. We assessed convergence to the true posterior distribution: (i) qualitatively through visual inspection of plots of the Markov chains for mixing and stationarity, as well as the corresponding density plots of the pooled posterior Markov chains for unimodality; and (ii) quantitatively using the Brooks-Gelman-Rubin (BGR) convergence statistic. The BGR factor is the ratio between *among-chain* and *within chain* variability (Brooks and Gelman, 1998). When the upper limits of the BGR factor are close to one, the chains have converged. The accuracy of the posterior parameter values was inspected by verifying that the Monte Carlo error (an estimate of the difference between the mean of the sampled values and the true posterior mean) for all parameters was less than 5% of the sample standard deviation (Spiegelhalter et al., 2003).

3. Results

3.1. Phosphorus loading

The relative TP and hydraulic loading contributions in Cootes Paradise marsh from 1996 to 2012 are shown in Fig. 2a, b. Spencer Creek is the greatest source of phosphorus, representing approximately 69% of the tributary loading, as well as an average of 24% and 58% of TP and hydraulic loading received during the growing season, respectively. Urban runoff is the second most important source, accounting for 30% of TP loading. The Dundas WWTP and CSOs each represent 17% of the TP loading discharged into the marsh. Notwithstanding the uncertain

effectiveness of CSO containment as the main CSO tank has been significantly leaking since 2014, the WWTP's relative contribution may have become even higher after the substantial capture and treatment of CSOs since 2013. A typical practice when calculating the contribution of point sources is to postulate a constant nutrient concentration for effluent, which does not hold true for the Dundas WWTP (Fig. 2c, d). Based on registered concentrations and flows from 2005 to 2016, there is considerably higher within- and among-year variability with respect to TP concentrations than flows. In eutrophication management, net loading ($= \text{Flows}_{\text{exogenous}} \times [\text{TP}_{\text{exogenous}} - \text{TP}_{\text{Cootes}}]$) can more comprehensively account for the role of different exogenous nutrient sources since it weighs the displacement of phosphorus against the variability of the corresponding flow regimes. Net loading is calculated by multiplying the inflows from a particular source with the difference between the inflow and outflow concentrations. Simply put, net loading accommodates the

idea that two equal total loads with opposite pairs of flow and concentration –high flow with low concentration or low flow with high concentration– could potentially have very different effects on the trophic state of the system. The recorded values suggest that net loading contribution from Dundas WWTP generally remains positive. That is, effluent concentrations ($244 \pm 199 \mu\text{g TP L}^{-1}$) tend to be higher than the ambient levels ($202 \pm 119 \mu\text{g TP L}^{-1}$) in West Pond. The actual flow values ($14.7 \cdot 10^3 \text{ m}^3 \text{ day}^{-1}$) and associated year-to-year variability ($1.84 \cdot 10^3 \text{ m}^3 \text{ day}^{-1}$) suggest that flows can significantly modulate the residence of the phosphorus masses into the innermost segment (West Pond volume $\approx 28 \cdot 10^3 \text{ m}^3$) of Cootes Paradise marsh. Interestingly, the loading from the three major tributaries in the area (Spencer, Chedoke, and Borer's Creeks) display distinct seasonal patterns with significantly lower values registered from July to September (Fig. 2e).

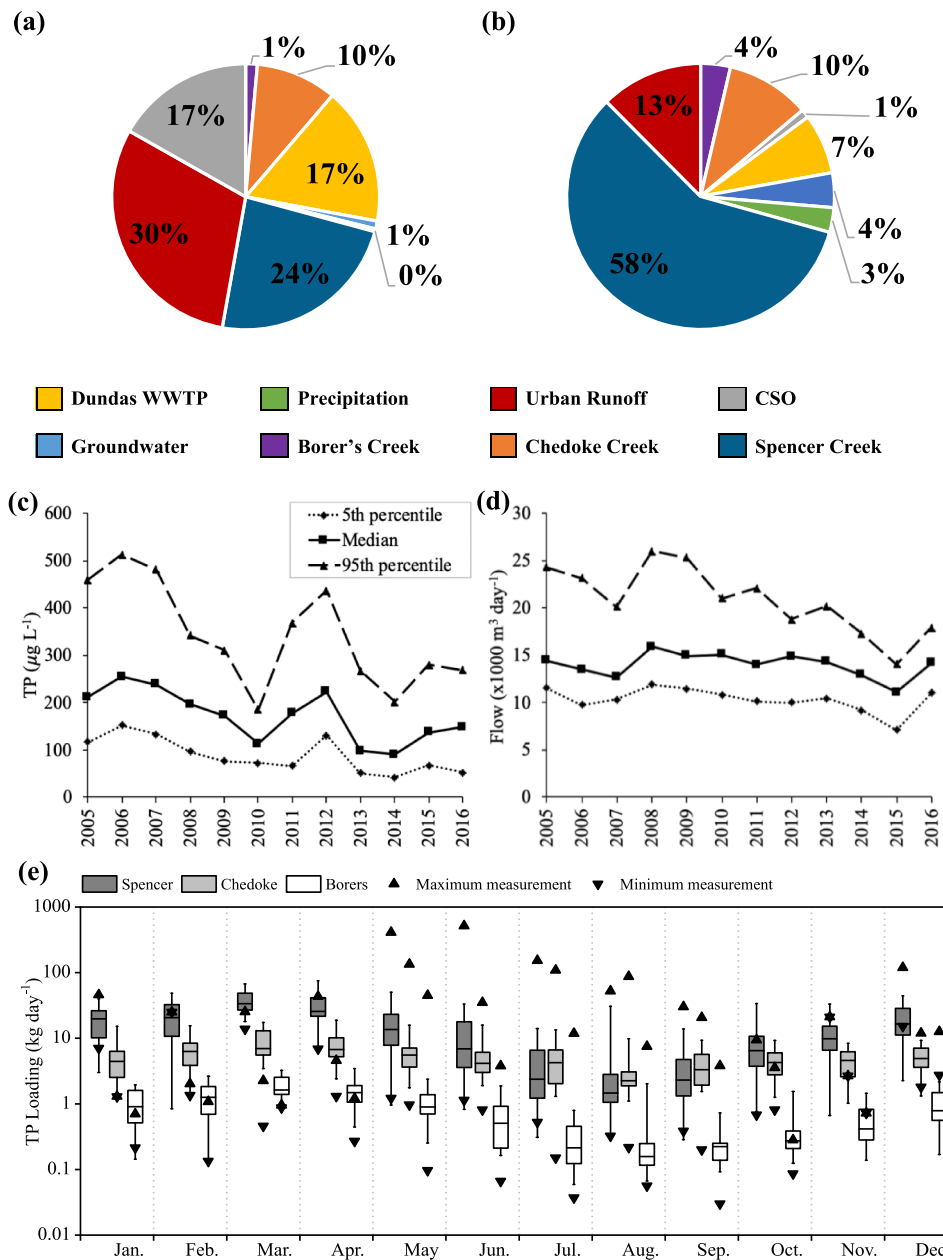


Fig. 2. TP loading and flow contributions into Cootes Paradise marsh during the growing season (May–October). (a) Daily TP loading and (b) flow contribution from point- and nonpoint-sources (1996–2012). (c) TP concentrations and (d) flow rates of effluent from Dundas WWTP (2005–2016). (e) Monthly averages of TP loading estimates (1996–2012) from the rating-curve method for the three major tributaries: Spencer, Chedoke and Borer's Creeks (Kim et al., 2016). Whiskers extend to the 5th and 95th percentiles. Triangles represent minimum and maximum registered loading values in each creek per month.

3.2. Mechanistic modelling

The model closely reproduced the seasonal TP and Chla concentrations in Cootes Paradise, but less so the monthly values of the same water quality variables (Kim et al., 2019). In particular, we found a satisfactory fit for the seasonal TP ($RE = 23.7\%$ and $RMSE = 54 \mu\text{g L}^{-1}$) and Chla values ($RE = 30.6\%$ and $RMSE = 16 \mu\text{g L}^{-1}$), but the resulting error was higher when model performance was evaluated against monthly TP ($RE = 54.7\%$ and $RMSE = 83 \mu\text{g L}^{-1}$) and Chla concentrations ($RE = 60.3\%$ and $RMSE = 29 \mu\text{g L}^{-1}$). Details of the year-to-year model performance, the parameter values assigned during the model calibration, and the resulting characterization of the major biogeochemical processes in Cootes Paradise marsh are presented in Kim et al. (2018, 2019). According to the simulated interplay among exogenous loading, autotrophic assemblage dynamics, and nutrient release from the sediments (Fig. S1), external TP loads contribute approximately 27.1 kg day^{-1} and are distinctly greater than the internal loading (i.e., TP fluxes associated with diffusive exchange between water column and the sediments, wind resuspension, and bacteria-mediated decomposition). In particular, phosphorus originating from diffusive sediment reflux and resuspension rates –on average– contribute to the water column 12.0 kg day^{-1} , whereas the mineralization of particulate matter merely corresponds to 0.75 kg day^{-1} . Our model suggests that approximately 6.2 kg day^{-1} are lost from the water column through sedimentation of biogenic or allochthonous material,

and 22.3 kg day^{-1} through outflows to Hamilton Harbour. There is also an additional 6.9 kg day^{-1} of phosphorus sequestered in phytoplankton cells that is exported through the outflows from the marsh. The permanent loss of phosphorus from the system through burial to deeper sediments accounts for 2.3 kg day^{-1} , resulting in a net phosphorus flux (sedimentation + macrophyte mortality - sediment reflux/ resuspension - macrophyte uptake - burial) of 9.2 kg day^{-1} from the sediments (Fig. S1).

Given their current low abundance levels in the system, macrophytes appear to play a minor role in the phosphorus cycle, removing a net amount of only 1.3 kg day^{-1} from the sediments and contributing 0.3 kg day^{-1} into the water column through respiration and decomposition of aging plant tissues (Fig. S1). Nonetheless, Kim et al. (2018, 2019) predicted that the role of macrophytes could be critical in inducing a non-linear regime shift to a more desirable ecological state, contingent upon the extent of their proliferation into the system and their ability to sequester phosphorus from the water column. Consistent with the latter finding, the present analysis suggests that a distinct decline in ambient Chla levels could result from the coupled effect of an elevated submerged macrophyte density (and associated P sequestration) and Dundas WWTP upgrades to reduce point-source loading into the innermost area of Cootes Paradise (Fig. 3 and Figs. S2-S3). In particular, we examined the change in the ambient Chla levels in response to the following point-source loading scenarios: (i) 2006 represents the year with the worst conditions in terms of the Dundas WWTP

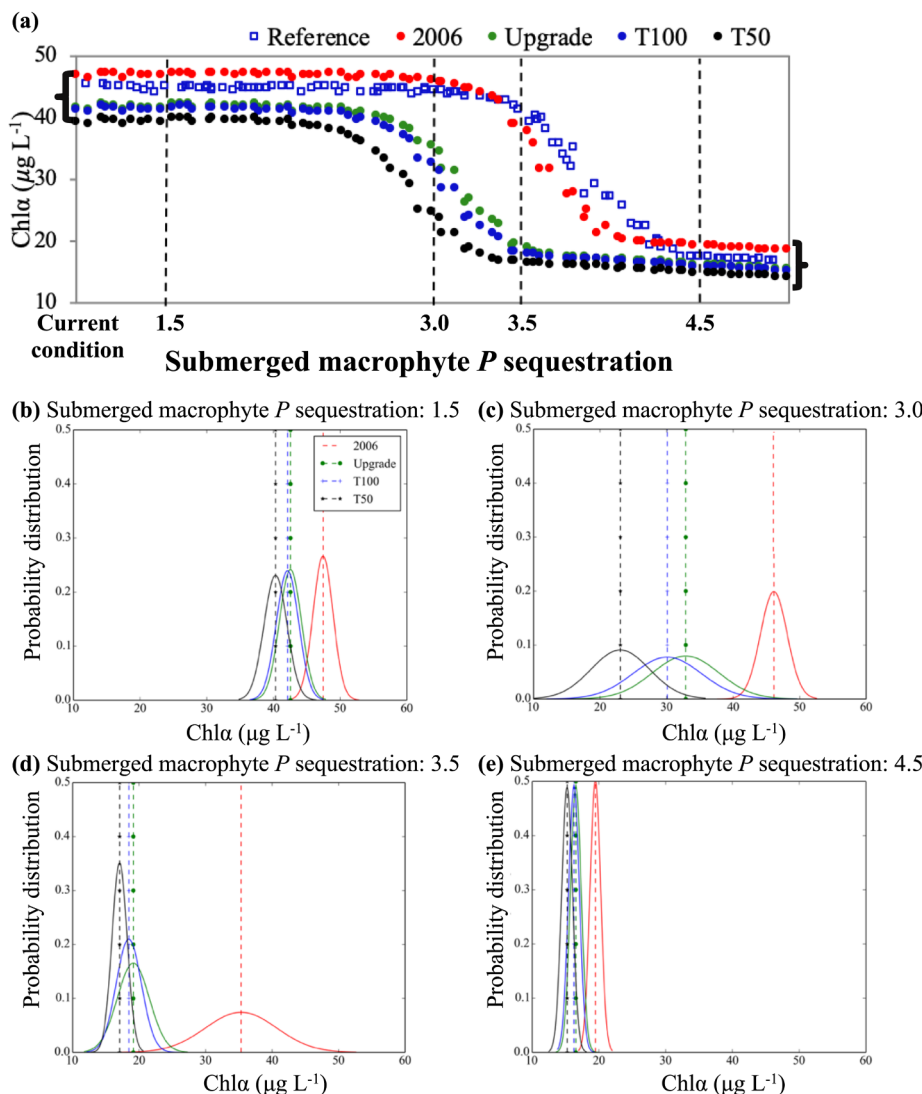


Fig. 3. (a-e) Predictive distributions of seasonal Chla concentrations average over the 2008–2012 period in response to different Dundas WWTP loading scenarios and varying degrees of P sequestered by the submerged aquatic vegetation. The latter process was emulated by the combined variation of respiration ($0.0120\text{--}0.0150 \text{ day}^{-1}$) and mortality ($0.0384\text{--}0.0480 \text{ day}^{-1}$) of submerged macrophytes, and P quota in macrophyte biomass. The numbers in the x-axis of the top panel represent the multipliers used to increase the strength of P sequestration relative to the reference conditions ($0.0025 \text{ g P g DW}^{-1}$) assigned by Kim et al. (2019), e.g., 1.5, 3, 3.5, and 4.5 reflect P quotas in plant tissues equal to 0.00375 , 0.0075 , 0.00875 , and $0.01125 \text{ g P g DW}^{-1}$. The uncertainty of Chla concentrations stems from the variability associated with the non-point source loading, which was simulated by inducing $\pm 15\%$ perturbations to the present conditions.

performance between 2005 and 2016; (ii) the *Upgrade* scenario is based on the 2013 conditions when the Dundas WWTP upgrades were completed; (iii) *T100* represents an additional improvement targeting *TP* effluent concentrations of $100 \mu\text{g L}^{-1}$; (iv) *T50* refers to a *TP* effluent target of $50 \mu\text{g L}^{-1}$; and (v) the *Reference* scenario reflects the prevailing conditions used to force the model during our calibration exercise (Kim et al., 2019). To simulate the effect of *P* sequestration by a growing submerged macrophyte community, we applied a multiplier to reduce submerged macrophyte respiration and mortality rates (in 5% increments) and increase the *P:C* ratio in their biomass relative to current conditions. A multiplier of one reflects the current conditions (calibrated values), while a multiplier of two represents a more prosperous submerged macrophyte community through the reduction of mortality and respiration losses by 10% ($= 2 \times 5\%$) along with a twofold increase in the amount of *P* stored in their biomass relative to current conditions. One interesting result from this exercise is that the specification of critical macrophyte-ecophysiological processes alone (*P* sequestration and metabolic losses) can trigger the emergence of either phytoplankton-dominated or macrophyte-dominated states, which appear to be fairly resilient with respect to the capacity of WWTP nutrient loading variability to induce dramatic changes to the prevailing water quality conditions (i.e., see the ranges that correspond to the brackets on the left and right ends of Fig. 3a). Similar to Kim et al. (2018), we identified a critical range of submerged-macrophyte characterizations (i.e., the area corresponding to macrophyte *P* quotas from 0.0075 to $0.00875 \text{ g P g DW}^{-1}$) between the two extreme states, in which the state of the macrophyte community (i.e., a threshold biomass density and associated impact on *P* cycle) can maximize water quality improvements from management actions in the watershed. Under these conditions, the desirable shift to an alternative ecological state ($< 20 \mu\text{g Chla L}^{-1}$) not only could occur with the most aggressive nutrient-loading reduction scenarios (*T100*, *T50*), but also with the current WWTP upgrades implemented in 2013 (*Upgrade*).

3.3. Statistical modelling

The first model in our feedforward data-driven framework displayed satisfactory performance with low posterior standard error (σ_{WP}) of 0.36 ± 0.02 , i.e., median model error of $1.43 \mu\text{g TP L}^{-1}$ with a 95% credible interval (or 95% CI) between $1.38\text{--}1.48 \mu\text{g TP L}^{-1}$, but the coefficient of determination ($r^2 = 0.17$) between measured and predicted median concentrations was fairly low (Table S1). The signal-to-noise ratios of the regression coefficients β_{WP1} (0.34 ± 0.05) and β_{WP2} (-0.18 ± 0.17) suggested that the *TP* concentrations of the treated sewage from Dundas WWTP have a distinct signature on the ambient *TP* levels registered in West Pond, but (counter to our previous assertion) the corresponding flows have a moderately strong signature on the contemporaneous ambient *TP* levels in West Pond despite their capacity to modulate the flushing rates in the same segment (Fig. 4 and Table S1). The second model in our feedforward system predicted the *TP* concentrations in the western area of the main marsh, Cootes-West, satisfactorily with a low posterior standard error (σ_{WP}) of 0.34 ± 0.02 , and high $r^2 = 0.73$ (Table S1). The signal-to-noise ratios of the corresponding model parameters indicated a strong positive relationship between the ambient *TP* in the western marsh and the *TP* concentrations in Spencer Creek ($\beta_{CW2} = 0.25 \pm 0.04$), and less so those with West Pond ($\beta_{CW1} = 0.12 \pm 0.07$). The same model highlights the predominant role of the hydraulic loading of Spencer Creek in shaping the flushing rates in the western segment of the marsh ($\beta_{CW2} = -0.41 \pm 0.02$). In the central marsh, Cootes-Centre, the TP_{CC} and $Chla_{CC}$ models were characterized by low standard error values ($\sigma_{CC} = 0.41 \pm 0.02$ and $\tau_{CC} = 0.07 \pm 0.04$) and satisfactory r^2 values (≥ 0.41). According to these models, ambient *TP* levels are strongly influenced by those prevailing at the preceding segment, Cootes-West ($\beta_{CC1} = 0.24 \pm 0.07$), and subsequently determine the level of phytoplankton biomass ($\gamma_{CC1} = 0.60 \pm 0.18$) at Cootes-Centre, whereas the *TP* concentrations registered at the Westdale inlet have a weaker

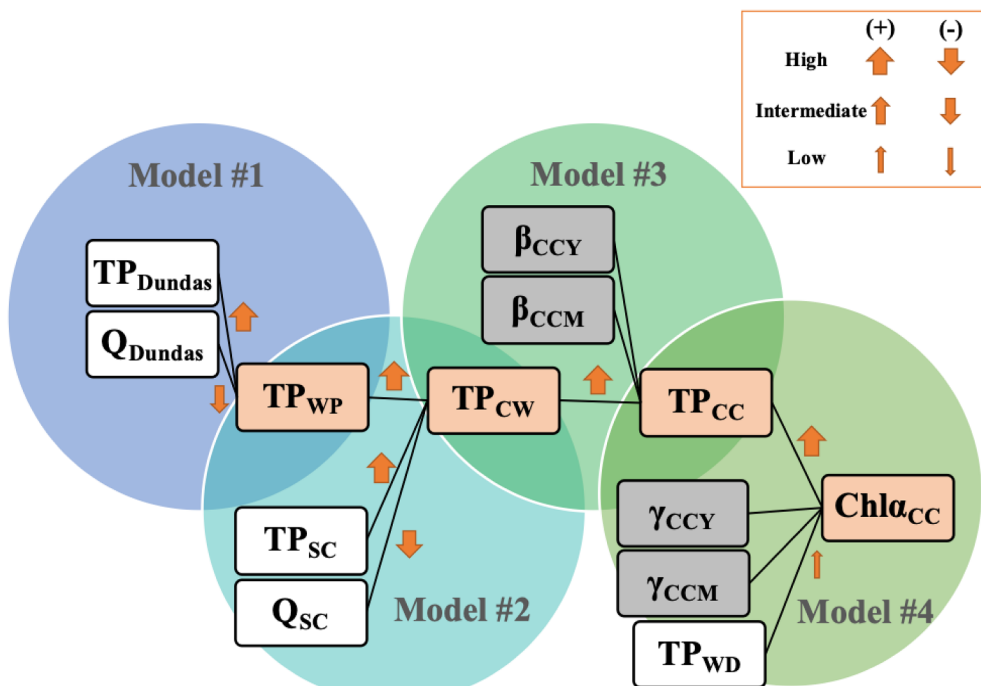


Fig. 4. Conceptual diagram of our statistical modelling framework. Orange boxes represent response variables of each of the statistical models, which also serve as explanatory variables for subsequent models. Gray boxes represent model intercepts. β_{CCY} and β_{CCM} correspond to the year- and month-specific intercepts that accommodate among- and within-year variability for predicting TP_{CC} , respectively. γ_{CCY} and γ_{CCM} correspond to the year- and month-specific intercepts that accommodate among- and within-year variability for predicting $Chla_{CC}$, respectively. Upward (downward) arrows indicate positive (negative) relationships between the corresponding predictor and response variables. Bivariate relationships were categorized into three groups based on the posterior probabilities of their respective slope regression coefficients to be positive/negative (strong: $\geq 95\%$, intermediate: $< 95\%$ and $\geq 85\%$, weak: $< 85\%$ and $\geq 75\%$).

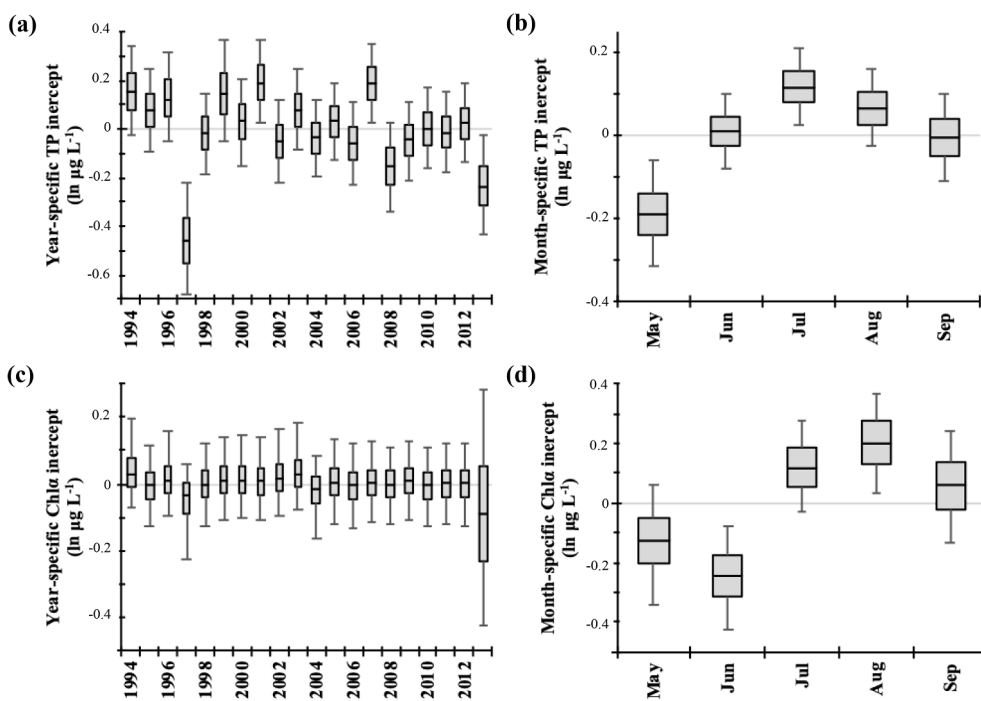


Fig. 5. Year- and month-specific intercepts of the TP and Chl α models that accommodate among- and within-year variability in the central area of Cootes Paradise marsh during the 1994–2013 period. The whiskers delineate the 90% credible intervals.

signature ($\gamma_{CC2} = 0.16 \pm 0.21$). The intercept terms, for the year-to-year variability in the central area, indicate a declining TP trend and a lack of a long-term Chl α pattern during the 1994–2013 period (Fig. 5a, c). Interestingly, the terms were able to capture the atypically low TP concentrations that prevailed in 1997, as well as the particularly high concentrations registered in 2007 (Fig. 5a and Table S2). The latter record was the result of a major pesticide spill that killed 5–15 million fish, and their tissue decomposition on the sediment bottom that

profoundly elevated nutrient levels (Theysmeijer and Galbraith, 2007). Moreover, there is evidence of strong seasonal patterns for TP and Chl α concentrations with the annual maxima typically occurring in July and August, respectively (Fig. 5b, d and Table S3).

Following the sequence of cause-effect relationships that formed the foundation of our statistical modelling framework, we can infer that TP concentrations in West Pond typically vary from 150 to 220 $\mu\text{g L}^{-1}$ and lead to ambient TP levels in the western end of the marsh that can range

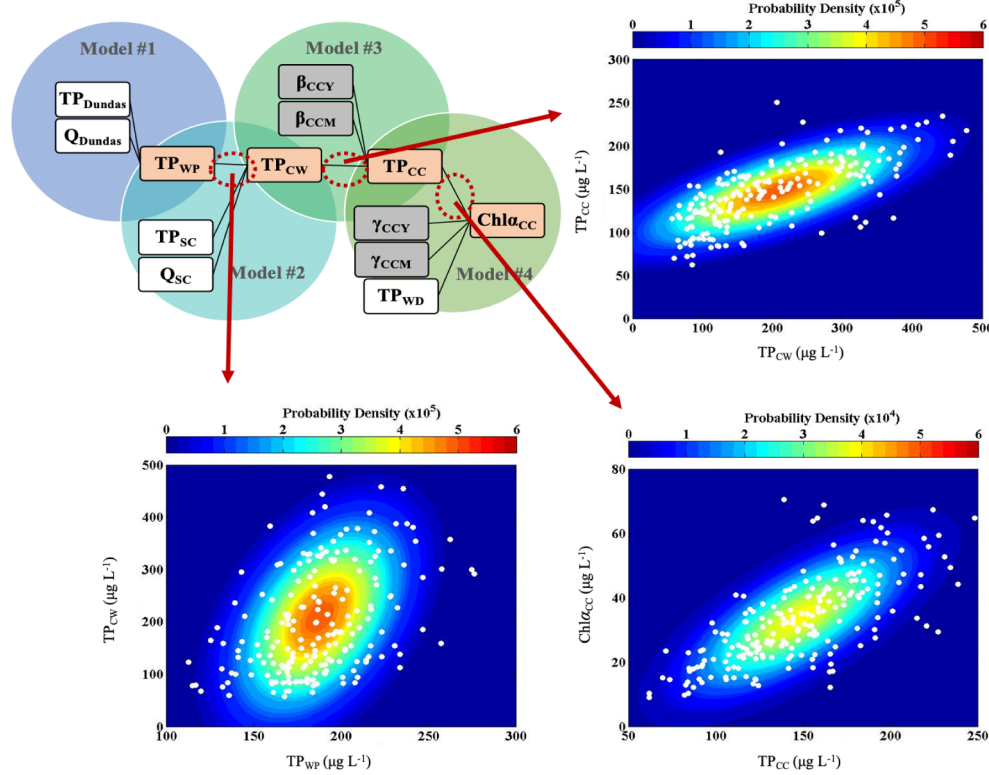


Fig. 6. Posterior joint distributions linking the ambient TP levels at the innermost segment (TP_{WP}) of Cootes Paradise marsh with those prevailing at the western area (TP_{CW}), and subsequently the latter ones (TP_{CW}) with those at the central (TP_{CC}) area. The last panel shows the joint distribution of TP (TP_{CC}) and Chl α ($Chl\alpha_{CC}$) concentrations in the central segment. White dots represent the mean posterior predictions drawn from our statistical modelling framework that were used to recreate the joint distributions.

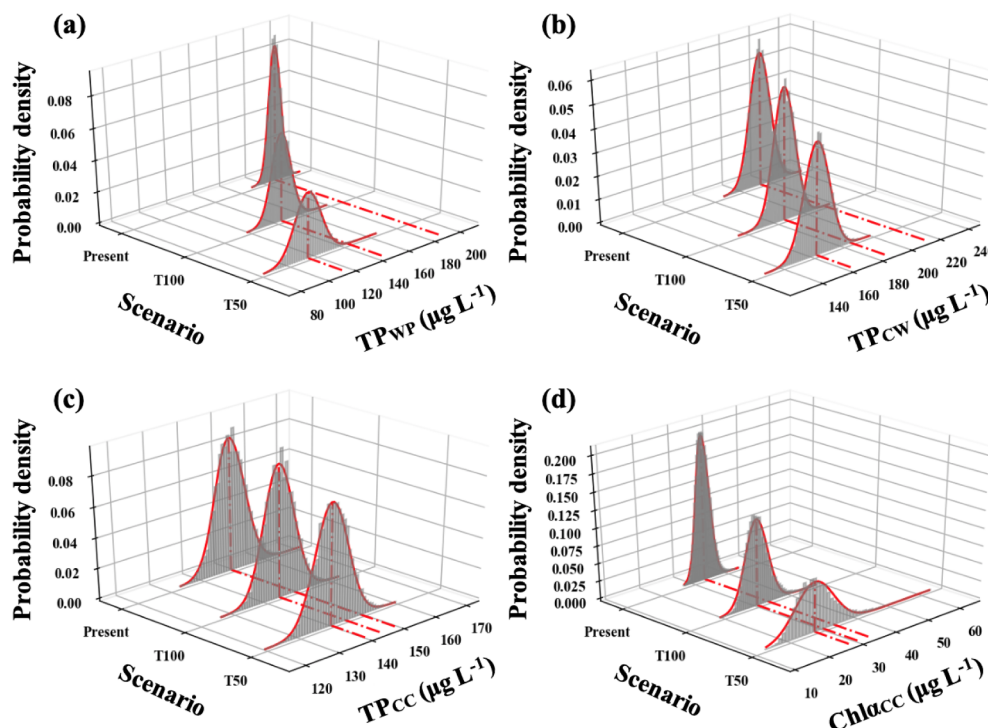


Fig. 7. Predictive distributions of seasonal TP concentrations in the (a) innermost, (b) western, and (c) central area of Cootes Paradise marsh based on different loading conditions from Dundas WWTP. Present refers to the prevailing conditions during the 1994–2013 period; T100 represents an average TP effluent concentration equal to $100 \mu\text{g L}^{-1}$; T50 represents an average TP effluent concentration equal to $50 \mu\text{g L}^{-1}$. Panel (d) shows the predictive distributions of seasonal Chlacc concentrations in the central area of Cootes Paradise marsh based on the same loading scenarios.

from 100 to $300 \mu\text{g L}^{-1}$ (see green-orange-red colored areas with higher probability density values in Fig. 6). The wide range of the latter concentrations reflects the fact that Spencer Creek, through its dual role (i.e., inflowing non-point source nutrients, hydraulic loading), can profoundly modulate the water quality in the marsh's western end regardless of the amount of nutrients transported from West Pond. In spite of the substantial variability characterizing the western end of Cootes Paradise, the range between 100 to $150 \mu\text{g TP L}^{-1}$ registers the highest likelihood in the central area of the marsh, and subsequently leads to Chlacc concentrations that vary from 20 to $50 \mu\text{g L}^{-1}$ (Fig. 6). Based on this general assessment, our analysis of nutrient loading scenarios predicts that the establishment of an average TP effluent concentrations of 100 and $50 \mu\text{g L}^{-1}$ (T100 and T50 scenarios, respectively) could reduce the average ambient TP levels in West Pond by 25% and 40%, respectively (Fig. 7). The same loading scenarios could also lead to an average 13% and 24% decrease of the TP concentrations in the western end of the main marsh, but their signals weaken in the central area. In particular, our feedforward model predicted that the ambient TP and Chlacc levels will decline by less than 7–8% with considerable variability surrounding these mean predictions (Fig. 7).

4. Discussion

A recent trend in the literature is the adoption of multi-model strategies that draw upon the complementary strengths of data-driven and mechanistic models to accommodate the wide range of conceptual and operational uncertainties that typically characterize modelling exercises (Arhonditsis et al., 2019a,b). Consistent with this practice, we used a spatially explicit model with an empirical basis to connect the water quality conditions in the innermost western segment with the western and subsequently with the central area of Cootes Paradise marsh. Owing to its simple structure, we were able to remain within the realms of data-based parameter estimation and elucidate several key cause-effect relationships among hydraulic loading, riverine/effluent TP concentrations, and ambient TP and Chlacc levels that shape the water quality conditions along the marsh. The statistical model, however, cannot adequately support ecological forecasts since it lacks the foundation to account for biogeochemical processes (e.g., resource

competition within the autotrophic assemblage, sediment diagenesis, bioturbation, decomposition of dead plant issues) that could conceivably become important within an open natural ecosystem under distinctly different management practices. It is in this context that WEM offered insights about the persistence of the current eutrophic state, the likelihood to capitalize upon additional nutrient loading reductions, and the mechanisms that favour the emergence of a critical threshold where an abrupt shift to an improved ecological state could occur.

Dundas WWTP and water quality conditions in West Pond: West Pond is the largest floodplain pond ($\approx 9 \text{ ha}$) linked to western Lake Ontario, occupying the northern side of the Spencer Creek delta within Cootes Paradise marsh where the water quality conditions are predominantly influenced by the wastewater discharges from Dundas WWTP (Theysmeijer and Bowman, 2017). Flows from the WWTP display year-to-year variability with an average discharge rate of just under $15 \times 10^3 \text{ m}^3 \text{ day}^{-1}$, which represents $> 95\%$ of the annual water input to West Pond. TP in West Pond had always ranged within hypereutrophic levels ($200\text{--}450 \mu\text{g L}^{-1}$). After the recent WWTP upgrades in 2013, TP concentrations declined to less than $150 \mu\text{g L}^{-1}$, but were still representative of a hypereutrophic system (Theysmeijer and Bowman, 2017). Moreover, since carp exclusion, water clarity in West Pond has regularly reached the bottom (pond depth is generally lower than 60 cm). Given that our statistical model spans the period from 1994 to 2013, the post-2013 water quality trends support our predictions that lower TP effluent concentrations could indeed result in a distinct decline of the ambient TP levels in West Pond. Another contributor to the recent water quality improvement in West Pond could have been its reconnection with the Spencer Creek in 2003, allowing creek water and fresh sediment to enter the pond during bank full flood events and potentially dilute/bury the highly enriched sediments from the Dundas WWTP discharges (Reddick and Theysmeijer, 2012).

The question arising though is to what extent does the predicted reduction of the average TP concentrations by an additional 15%, when effluent phosphorus is reduced from $100 \mu\text{g L}^{-1}$ (T100 scenario) to $50 \mu\text{g L}^{-1}$ (T50 scenario), justifies the substantial efforts (and costs) associated with the latter proposed upgrade. From an ecological standpoint, a plausible argument in favour of this change is that the effluent target of $50 \mu\text{g L}^{-1}$ would make the Dundas WWTP a negative

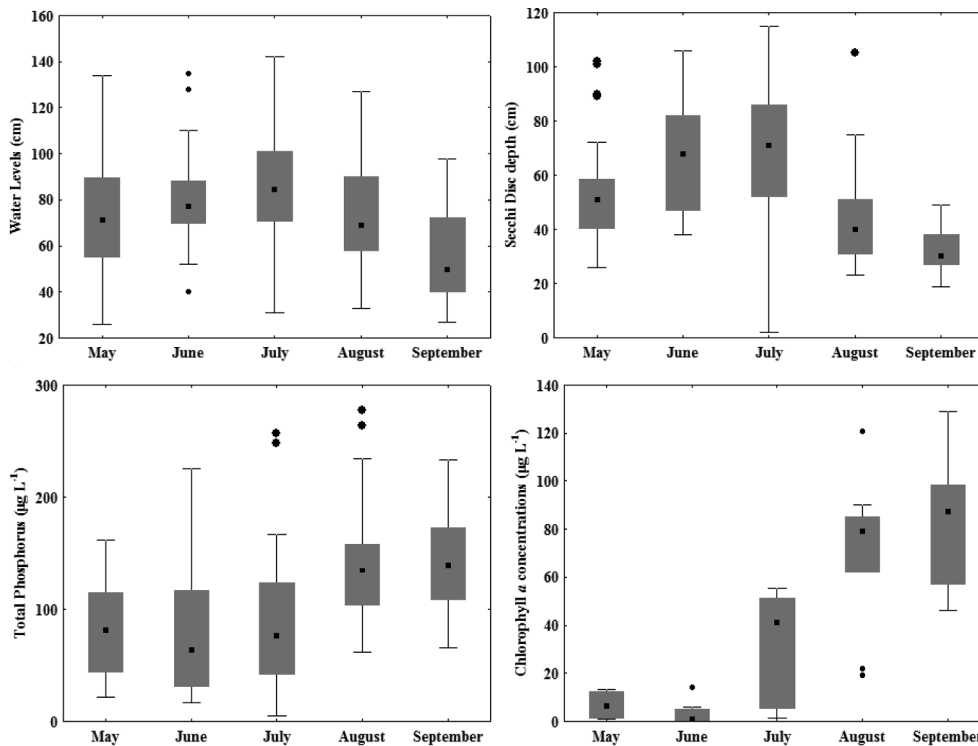


Fig. 8. Water levels, Secchi Disc depth, and TP and Chla concentrations in Cootes Paradise marsh during the 2014–2016 period. The registered water quality trends provide evidence of two distinct ecological states in the marsh within the same season. Details on the sampling network and monitoring results can be found in Mataya et al. (2017).

net loading source, and therefore the corresponding flows would decisively purify the water quality in West Pond, especially during dry summer conditions. This prospect is particularly important when we consider that sediment P levels remain above the lowest ($>0.6 \text{ mg g}^{-1}$) and –for the most part– severe effect ($>2 \text{ mg g}^{-1}$) levels, and have not shown a distinctly monotonic decline in West Pond since first measured in 1975 (see Fig. 8 in Theysmeyer and Bowman, 2017). It is also important to keep in mind that the areal point-source loading rate at Cootes Paradise marsh ($1.4 \text{ kg km}^{-2} \text{ day}^{-1}$) is multiple times greater than the rate at the Bay of Quinte ($0.05 \text{ kg km}^{-2} \text{ day}^{-1}$); a neighbouring eutrophic embayment on the northeastern shore of Lake Ontario (Arhonditsis et al., 2016). Areas that are particularly affected by the Dundas WWTP also display elevated levels of unionized ammonia, which is a highly toxic compound with guidelines for aquatic life set at $19 \mu\text{g L}^{-1}$, and some heavy metal contamination (e.g., copper) (Theysmeyer and Bowman, 2017). It is also worth noting that a full characterization of the effluents is still missing, which can contain a variety of heavy metals, organics, and salts (e.g., endocrine disruptors, pharmaceutical, and cosmetic products) with potentially deleterious effects on the aquatic biota, including the resurgence of the native flora and fauna (DeSolla et al., 1998; Harrison and Theysmeyer, 2014; Hughes et al., 2016).

Non-point source loading and water quality in Cootes Paradise marsh: Being a major contributor of TP (24%) and hydraulic (56%) loading, our study identified Spencer Creek as a critical non-point source that modulates the prevailing water quality conditions in the marsh. This tributary drains an area of 230 km^2 with 47% occupied by agricultural and pasture, and 28% occupied by forests. Spencer Creek inflows are consistently the best quality water entering the marsh, and the corresponding total suspended solids and TP concentrations have dropped dramatically after carp were excluded from the system (Reddick and Theysmeyer, 2012). Our modelling analysis showed that hydraulic loading from Spencer Creek could be the single most important driver of the residence time of riverine nutrient fluxes, as well as those entering the western area of Cootes Paradise from West Pond. The relative importance of the latter mechanism has shown to vary significantly within the year: Flow discharge rates from Spencer Creek

can vary from $4.59 \pm 1.86 \text{ m}^3 \text{ s}^{-1}$ in March to $0.57 \pm 0.77 \text{ m}^3 \text{ s}^{-1}$ in August. Interestingly, the monthly ambient TP levels typically range from 40 to $80 \mu\text{g L}^{-1}$ during the summer months, but remain consistently higher than the targeted TP threshold of $30 \mu\text{g L}^{-1}$ (Reddick and Theysmeyer, 2012). These fairly low TP concentrations registered in Spencer Creek reinforce the idea that its net loading contribution has mostly been negative, and therefore the inflowing water masses can alleviate the eutrophication severity by carrying away some of the excess internal and/or point-source loads (Kim et al., 2016).

Although Spencer Creek accounts for the greatest amount of phosphorus input of the three major tributaries in the area, Chedoke Creek is responsible for approximately four times higher areal phosphorus loading (Theysmeyer et al., 2009). Chedoke Creek drains a highly urbanized 20 km^2 watershed that periodically receives sewage from several CSOs, while increased precipitation in recent years has negatively affected water quality, causing additional sewer overflows and urban runoff (Reddick and Theysmeyer, 2012). Owing to data limitations, we were unable to explicitly consider the impact of Chedoke Creek on the prevailing water quality conditions of the marsh with our statistical model, but a sensitivity analysis exercise with the mechanistic model presented by Kim et al. (2016) indicated that TP loading from Chedoke Creek is comparable with the TP loads from other non-point sources (e.g., urban runoff). Consistent with this evidence, Dong et al. (2019) predicted that the continued deforestation and urbanization trends in the Cootes Paradise and Hamilton Harbour watersheds will likely trigger a series of changes in the water cycle, including the increased frequency of peak flow events, decreased evapotranspiration, greater surface runoff, and loss of hydrological stationarity (Mao and Cherkauer, 2009; Trudeau and Richardson, 2016). Moreover, recent research in the Hamilton Harbour watershed has shown that both TP and phosphate loads can vary by three orders of magnitude between wet and dry conditions, with storm events and spring freshets driving peak daily loads in urban and agricultural catchments, respectively (Long et al., 2014; 2015). Importantly, a significant fraction ($>50\%$) of the annual phosphorus loads can be generated during a small number of brief but intense precipitation events (Long et al., 2015). Similar patterns have also been reported by Reddick and Theysmeyer (2012), who

noted that water quality in Spencer Creek temporarily declines during heavier rains because of increased runoff from the land and a sewer-overflow connection. Thus, although non-point source loading on a monthly or seasonal basis may not be conducive to alleviating eutrophication symptoms in the receiving waterbody, the devastating impacts of rare but extreme/high-intensity events (i.e., individual storm events) cannot be ruled out and requires consideration from the on-going management efforts, especially if deforestation and urbanization trends in the area continue (Trolle et al., 2019).

Characterization of the role of macrophytes and internal loading mechanisms: Drawing upon the available data, our statistical modelling framework suggested that the loading reductions from Dundas WWTP will improve the water quality conditions in the marsh, but they cannot single-handedly trigger an abrupt shift to an alternative, clear-water state. The additional insights gained by the mechanistic model showed that an important condition for the realization of such a “tipping” point largely depends on the presence of a thriving macrophyte community with an augmented ability to sequester phosphorus. Consistent with recent empirical and theoretical evidence (Thomasen and Chow-Fraser, 2012; Theysmeijer et al., 2016; Kim et al., 2016; 2018), our mechanistic model predicted that macrophytes play a minimal role in the phosphorus budget of Cootes Paradise marsh during the simulated (1996–2012) period, reflecting their low abundance (biomass and density) and slow resurgence. In addition to the degraded inflowing water, carp activity, dominance by non-native macrophyte species, and water level regulations represent fundamental challenges for the restoration of macrophytes in the wetland. In particular, the non-native Eurasian manna grass (*Glyceria maxima*) and common reed (*Phragmites australis*) predominantly occupy the meadow marsh habitat zone and outcompete the native species (Theysmeijer et al., 2016). Water cycle variations in Lake Ontario maintain fairly high summer water levels in the marsh, thereby preventing natural emergent marsh reestablishment from seedlings (Chow-Fraser, 2005). Physical destruction of plant communities by carp activity (>10% of the total catch of large fish in 2016) coupled with higher turbidity prevent light penetration to the bottom and hamper submerged vegetation growth (Lougeed et al., 2004). The prevalence of a poorly illuminated environment also renders a competitive advantage for phytoplankton that are typically dominated by genera of cryptomonads (*Cryptomonas*, *Rhodomonas*) and euglenophytes (*Euglena*, *Lepocinclis*, *Phacus*), which are known to display greater adaptation to turbid and low-light conditions (Chow-Fraser et al., 1998; Kim et al., 2018).

Recognizing that a complex interplay among physical, chemical, and biological mechanisms bolsters the persistence of the current impaired state and lessens the likelihood of submerged aquatic vegetation resurgence, the areal expansion of aquatic vegetation through on-going restoration plans (60 ha in the 1990s, 133 ha in 2015, and 270 ha set as the latest objective) is a critical remedial measure for the marsh's ecological status (Theysmeijer et al., 2016). Specifically, the local management actions at Cootes Paradise marsh prioritize the plantings of emergent plants, mainly cattails (*Typha* sp.) in the Spencer Creek delta area, and less so meadow, like lake-bank sedge (*Carex lacustris*), and submerged macrophytes, such as white water lilies (*Nymphaea odorata*) (Reddick and Theysmeijer, 2012). The boundary between the perennial emergent marsh and submerged vegetation is determined by the water cycle, whereby massive emergent seedling germination in the exposed summer mudflat is mainly favoured by a maximum summer water level less than 74.75 mean sea level (Chow-Fraser, 2005). Nonetheless, owing to the sustained high water levels in Lake Ontario over the past 30 years, this condition has been rarely met in Cootes Paradise marsh and therefore, a significant portion ($\approx 25\%$) of the shoreline still lacks emergent vegetation with dire ramifications for the erosion intensity in the marsh (Theysmeijer et al., 2016). Because of the challenges posed by invasive plant species and water level fluctuations, both the intensification of planting efforts and the control of common reed and manna grass populations represent two critical actions that

should continue in order to re-establish the targeted plant species in their native marsh habitats.

Restoration of emergent and meadow macrophytes in Cootes Paradise could also increase the resilience of submerged macrophytes and mediate their proliferation through a series of synergistic mechanisms, such as stabilization of the sediments, improved water clarity, and increased competition with the algal assemblage (Theysmeijer et al., 2016; Kim et al., 2018). Under the presence of a thriving emergent/meadow macrophyte community, Kim et al. (2018) showed that submerged plants can reach critical biomass density levels and more effectively compete against a wide range of characterizations of the phytoplankton assemblage. Regarding the factors that could conceivably shape the macrophyte-phytoplankton competition for nutrient procurement, it should be noted that our simulations do not accommodate the fact that macrophytes are covered by an active epiphyte community characterized by higher nutrient uptake per area rates (Howard-Williams and Allanson, 1981). Instead, we postulated a predominantly acropetal translocation movement, through which phosphorus uptake of submerged macrophytes takes place primarily from the sediment via their roots and less so from the water via their leaves (Granéli and Solander, 1988). Combined with a suite of traits that maximize P sequestration, the latter ecophysiological strategy has been shown to enable submerged plants to reach critical biomass density levels and become viable competitors within the autotrophic assemblage (Kim et al., 2018; 2019). Interestingly, dominant species of the Pondweed family, including *Potamogeton foliosus*, have recently displayed the ability to spread aggressively in the shallow, slow-moving waters of the marsh at the beginning of the growing season, thereby occupying the two thirds of the main marsh and greatly improving the water clarity and general water quality (Mataya et al., 2017). This elevated submerged macrophyte growth is short-lived and the plants start senescing by early July. Following their die-off, submerged aquatic vegetation growth is smothered by algae and remains sparse, while the microbial decomposition of the dead plant tissues dramatically deteriorates water quality conditions toward the end of the growing season, i.e., $TP > 150 \mu\text{g L}^{-1}$ and $\text{Chla} > 100 \mu\text{g L}^{-1}$ (Mataya et al., 2017).

Based on previous evidence from the system, we can infer that the restoration actions (i.e., nutrient loading reduction, macrophyte plantings, shoreline stabilization) in Cootes Paradise have brought the system closer to the tipping point, where a distinct water quality improvement could occur, but that threshold has yet to be decisively crossed to establish the resilient clear, macrophyte-dominated state. With that possibility in mind, one critical piece of information to determine the scale of the management efforts required to reliably restore the wetland is the quantification of the absolute and relative magnitude of internal nutrient loading. Consistent with empirical and theoretical estimates (Kelton and Chow-Fraser, 2005; Mayer et al., 2005; Kim et al., 2016), our mechanistic model predicted that internal P loading accounts for 12.0 kg day^{-1} , stemming from sediment reflux (4.9 kg day^{-1}) and wind resuspension (7.1 kg day^{-1}), which represents 30–35% of the TP loading into Cootes Paradise marsh. The internal diffusive fluxes from the sediment, as well as the pore-water soluble reactive phosphorus concentration gradients (Kim et al., 2019) are comparable with the values registered in the Bay of Quite (Markovic et al., 2019). Drawing parallels with other shallow aquatic environments, Cootes Paradise marsh will likely experience short-term summer pulses of increased mobilization of labile P forms (e.g., freshly deposited algal cells, redox sensitive P, polyphosphate) associated with intermittent changes in redox conditions and phytoplankton dynamics (Tammeorg et al., 2015; Parsons et al., 2017; Markovic et al., 2019). Nonetheless, Parsons et al. (2017) downplayed the likelihood of excessive P release during short-term anoxic periods in the system for two primary reasons: (i) owing to WWTP effluents and variable residence time with changing marsh water levels, nitrate (NO_3^-) levels are fairly high in the system, ranging anywhere from 30 to 80 mg L^{-1} (West Pond and Desjardins Canal) to 1 mg L^{-1} (main body of Cootes Paradise

marsh), and thus the apparent requirement for complete nitrate depletion prior to anoxia-promoted *P* release to the aqueous phase is rarely met; and (ii) the short-term redox fluctuations do not seem to trigger significant *P* remobilization to the aqueous phase of sediments due to the presence of mechanisms of reversible redistribution of both reduced iron (Fe^{+2}) and associated *P* within the solid phase, such as mineralogical phosphate immobilization and scavenging by anaerobic heterotrophic respiration.

Other potentially important internal sources of nutrients include the foliar release of phosphorus by actively growing and healthy macrophytes, as well as the leachable *P* pool or the decaying plant tissues returned into the water column through microbial decomposition (Gabrielson et al., 1984; Granéli and Solander, 1988; Herb and Stefan, 2003). While the former pathway is not considered to be a significant contributor, the latter one could play a significant role within both short- (rapid initial loss of phosphorus due to leaching) and long- (microbially mediated release of refractory organic phosphorus) time scales (Carpenter, 1981; Granéli and Solander, 1988). In particular, the bacterial decomposition of plant tissues is accelerated by higher temperatures, and is more pronounced in submerged plants (low cellulose content, richer root system) than in emergent macrophytes (perennial storage organs for carbohydrates and supporting tissues, which are resistant to microbial activity) (Twilley et al., 2019; Granéli and Solander, 1988; Leisti et al., 2016). This nutrient recycling pathway coupled with the direct effects of lower water levels on nutrient concentrations towards the end of the growing season (lower dilution, greater wind-driven stirring of the sediments) can explain the aforementioned pattern, whereby two distinct water quality states manifests in the marsh within the same season (Fig. 8). Namely, due to the inability of submerged vegetation to be sustained for a long time in the system, the low-nutrient, clear-water state at the beginning of the growing season is rapidly succeeded by a phytoplankton-dominated state, where the nutrient concentrations are further elevated by the decomposition of the dead plant tissues and the gradual lowering of water levels (70–90 cm seasonal fluctuations) in the marsh.

Uncertainty in the decision-making process and economic values of ecosystem services: Ecosystem services are the benefits that humans directly or indirectly gain from ecosystem functions, and thus this concept effectively links their structural and functional integrity with human welfare (Costanza et al., 1997). Knowledge of the value of ecosystem services in monetary terms is critical when considering trade-offs among costly and diverse policy decisions. In the present study, recognizing that the considerable uncertainties of our water quality predictions are associated with the role of a wide array of abiotic factors/biogeochemical mechanisms that cannot be easily controlled or mitigated (e.g., likelihood of macrophyte resurgence, sediment diagenesis, water level regulations, invasive species), we believe that the decision-making process can be meaningfully supported by a rigorous assessment of the economic benefits gained from a well-functioning ecosystem. Simply put, the decisions regarding the degree of investment of taxpayers' money to support the local restoration actions in Cootes Paradise marsh should not be determined solely by predictions of environmental quality goals that cannot unequivocally prove their achievability (e.g., Fig. 7), but also from the socioeconomic benefits of having a healthy ecosystem that is able to protect the integrity of native biotic communities and human wellbeing (Pascual et al., 2010; Allan et al., 2017).

The essence of any ecosystem service valuation exercise is the examination of the marginal improvement in ecosystem services that could be brought about by a policy change, in which the underlying expectation is that the total returns and benefits will be commensurate with (or higher than) costs and investments (Arhonditsis et al., 2019b). For example, Isely et al. (2018) estimated that a \$10 million investment to restore the Muskegon Lake Area of Concern would have a return on investment of approximately 6:1, or in other words, an added \$50 million in environmental value over a 20-year period due to increased

property prices and a more attractive recreational environment. Such a straightforward relationship between socioeconomic investments and environmental improvements may not hold true in the current state of Cootes Paradise marsh, considering that a wide array of ecological unknowns, feedback loops, and external factors shape its dynamics. Skeptical viewpoints could also claim that we have reached a point of diminishing returns, where the marginal benefits may not be worth the multimillion-dollar investments to future capital upgrades at the Dundas WWTP. In this regard, even though Cootes Paradise is a well-known socioecological hub in western Lake Ontario, it lacks a rigorous valuation of its ecosystem services. In a more general context, Troy and Bagstad (2013) found that the Great Lakes wetlands and their regulating services (e.g., nutrient regulation, soil retention, and flood control) have not received much attention in the literature. Through a spatially explicit value-transfer methodological framework to evaluate ecosystem services in Southern Ontario (Troy and Wilson, 2006), the same study concluded that the (often significant) cost of restoration of wetlands may be justified given the significant benefits delivered. Interestingly, Troy and Bagstad (2013) ranked Cootes Paradise marsh in the highest class ($> CAD\$20,000 \text{ ha}^{-1} \text{ year}^{-1}$ in 2011 prices) with respect to its average ecosystem service value (see their Fig. 5), even with the exclusion of important ecosystem services related to its role as a biodiversity/habitat refugium and cultural/recreational attraction. It is thus reasonable to assume that the total ecosystem service value of Cootes Paradise will be much higher relative to Troy and Bagstad's (2013) estimates, and consequently a precise knowledge of the benefits gained in monetary terms could offer support to keep the investments to environmental restoration going, despite the risk of falling short of the targeted environmental goals.

5. Conclusions

Combining the characterization of fundamental cause-effect, water-quality relationships, as depicted by a spatially explicit statistical model, with ecological forecasts drawn from a mechanistic model, the key findings of the present study regarding the likelihood of a clear, macrophyte-dominated state to emerge in Cootes Paradise marsh in the foreseeable future are as follows: (i) Nutrient loading reductions from Dundas WWTP will bring a significant water quality improvement in the innermost segment of Cootes Paradise (West Pond), but cannot single-handedly trigger a distinct shift to a desirable water quality state in the main marsh. (ii) Hydraulic loading from Spencer Creek is a predominant driver of the residence time of riverine nutrient fluxes, as well as those entering the western area of Cootes Paradise from West Pond. Recent local data show that surface runoff from agricultural areas are relatively pristine, thus highlighting the need to control nutrient pollution from urban areas in the Cootes Paradise watershed (Hamilton Conservation Authority, 2018). Best management practices within the surrounding agriculture-dominated watershed are also important for sustaining its net negative loading contribution, whereby the inflowing low-nutrient, water masses can alleviate the eutrophication severity by carrying away some of the excess internal and/or point-source loads; especially during the succeeding periods of episodic precipitation events. Minimizing non-point source loading will, therefore, require combined efforts to address nutrient export from urban areas (e.g., low impact development to increase rainwater infiltration and reduce runoff, effectiveness of CSO containment) and promote best management practices within agricultural areas. (iii) The anticipated realization of a "tipping" point, where an abrupt shift to an alternative ecological state could occur, depends on the presence of a thriving macrophyte community with ecophysiological attributes that magnify their ability to sequester phosphorus. (iv) Intensified local planting efforts and the control of invasive plant species represent two critical restoration actions that should continue in order to re-establish the targeted plant species in their native marsh habitats. Establishing a robust emergent/meadow macrophyte community in Cootes Paradise

marsh could also increase the resilience of submerged vegetation and mediate their proliferation through a series of synergistic mechanisms. (v) Internal loading (sediment diagenesis, wind resuspension, bioturbation) represents 30–35% of the total nutrient loading in the marsh, while the fluxes of regenerated nutrients from microbial decomposition of dead plant tissues could be responsible for the recent dramatic water quality deterioration in the marsh toward the end of the growing season. (vi) Viewing ecosystems as providers of economically valuable benefits to humans, our study advocates for the development of a rigorous framework that quantifies the importance of a well-functioning ecosystem in monetary terms as a critical piece of knowledge to guide the decision-making process in the face of uncertainty. Knowing the tangible economic benefits that could be gained from a successful ecosystem restoration is likely the most meaningful way to make management decisions when model predictions and available scientific understanding cannot unequivocally show that the targeted environmental quality goals will be met.

Acknowledgement

This project was undertaken with the financial support of the Government of Canada provided through the Department of the Environment and Climate Change (Great Lakes Sustainability Funds). We are grateful to Cheriene Vieira, Laud Matos, Duncan Boyd, Mark Bainbridge, Kristin O'Connor, Sarah Day, Julie Vanden Bylaardt, Margaret McIntosh, Murray Charlton, and Scott Millard for all their interest and support during this project.

Appendix A. Supplementary data

Supplementary data to this article can be found online at <https://doi.org/10.1016/j.ecolind.2019.105794>.

References

- Allan, J.D., Manning, N.F., Smith, S.D.P., Dickinson, C.E., Joseph, C.A., Pearsall, D.R., 2017. Ecosystem services of Lake Erie: spatial distribution and concordance of multiple services. *J. Great Lakes Res.* 43, 678–688. <https://doi.org/10.1016/j.jglr.2017.06.001>.
- Arhonditsis, G.B., Brett, M.T., 2005. Eutrophication model for Lake Washington (USA): Part I. Model description and sensitivity analysis. *Ecol. Modell.* 187, 140–178. <https://doi.org/10.1016/j.ecolmodel.2005.01.040>.
- Arhonditsis, G.B., Kim, D.-K., Shimoda, Y., Zhang, W., Watson, S., Mugalingam, S., Dittrich, M., Geater, K., McClure, C., Keene, B., Morley, A., Richards, A., Long, T., Rao, Y.R., Kalinauskas, R., 2016. Integration of best management practices in the Bay of Quinte watershed with the phosphorus dynamics in the receiving waterbody: what do the models predict? *Aquat. Ecosyst. Heal. Manag.* 19, 1–18. <https://doi.org/10.1080/14634988.2016.1130566>.
- Arhonditsis, G.B., Neumann, A., Shimoda, Y., Kim, D.-K., Dong, F., Onandia, G., Yang, C., Javed, A., Brady, M., Visha, A., Ni, F., Cheng, V., 2019a. Castles built on sand or predictive limnology in action? Part A: Evaluation of an integrated modelling framework to guide management implementation in Lake Erie. *Ecol. Inform.* 53, 100968. <https://doi.org/10.1016/j.ecoinf.2019.05.014>.
- Arhonditsis, G.B., Neumann, A., Shimoda, Y., Kim, D.-K., Dong, F., Onandia, G., Yang, C., Javed, A., Brady, M., Visha, A., Ni, F., Cheng, V., 2019b. Castles built on sand or predictive limnology in action? Part B: Designing the next monitoring-modelling-assessment cycle of adaptive management in Lake Erie. *Ecol. Inform.* 53, 100969. <https://doi.org/10.1016/j.ecoinf.2019.05.015>.
- Asaeda, T., Trung, V.K., Manatunge, J., 2000. Modeling the effects of macrophyte growth and decomposition on the nutrient budget in Shallow Lakes. *Aquat. Bot.* 68, 217–237. [https://doi.org/10.1016/S0304-3770\(00\)00123-6](https://doi.org/10.1016/S0304-3770(00)00123-6).
- Barbier, E.B., Acreman, M., Knowler, D., 1997. Economic valuation of wetlands: A guide for policy makers and planners. Ramsar Conservation Bureau, Gland, Switzerland.
- Brooks, S.P., Gelman, A., 1998. Alternative methods for monitoring convergence of iterative simulations. *J. Comput. Graph. Stat.* 7, 434–455.
- Carpenter, S.R., 1981. Submersed Vegetation: An Internal Factor in Lake Ecosystem Succession. *Am. Nat.* 118, 372–383.
- Chow-Fraser, P., 2005. Ecosystem response to changes in water level of Lake Ontario marshes: Lessons from the restoration of Cootes Paradise Marsh. *Hydrobiologia* 539, 189–204. <https://doi.org/10.1007/s10750-004-4868-1>.
- Chow-Fraser, P., Lougheed, V.L., Le Thiec, V., Crosbie, B., Simser, L., Lord, J., 1998. Long-term response of the biotic community to fluctuating water levels and changes in water quality in Cootes Paradise Marsh, a degraded coastal wetland of Lake Ontario. *Wetl. Ecol. Manag.* 6, 19–42. <https://doi.org/10.1023/A:1008491520668>.
- Christiansen, N.H., Andersen, F.O., Jensen, H.S., 2016. Phosphate uptake kinetics for four species of submerged freshwater macrophytes measured by a 33P phosphate radio-isotope technique. *Aquat. Bot.* 128, 58–67. <https://doi.org/10.1016/j.aquabot.2015.10.002>.
- Costanza, R., D'Arge, R., de Groot, R., Farber, S., Grasso, M., Hannon, B., Limburg, K., Naeem, S., O'Neill, R.V., Paruelo, J., Raskin, R.G., Sutton, P., van den Belt, M., 1997. The value of the world's ecosystem services and natural capital. *Nature* 387, 253–260. <https://doi.org/10.1038/387253a0>.
- Croft, M.V., Chow-Fraser, P., 2007. Use and development of the wetland macrophyte index to detect water quality impairment in fish habitat of Great Lakes coastal marshes. *J. Great Lakes Res.* 33, 172–197. [https://doi.org/10.3394/0380-1330\(2007\)33](https://doi.org/10.3394/0380-1330(2007)33).
- de Solla, S.R., Bishop, C.A., Van Der Kraak, G., Brooks, R.J., 1998. Impact of organochlorine contamination on levels of sex hormones and external morphology of common snapping turtles (*Chelydra serpentina serpentina*) in Ontario, Canada. *Environ. Health Perspect.* 106, 253–260. <https://doi.org/10.1289/ehp.98106253>.
- Dong, F., Neumann, A., Kim, D.-K., Huang, J., Arhonditsis, G.B., 2019. A season-specific, multi-site calibration strategy to study the hydrological cycle and the impact of extreme-flow events along an urban-to-agricultural gradient. [Submitted Manuscript].
- Gabrielson, J.O., Perkins, M.A., Welch, E.B., 1984. The uptake, translocation and release of phosphorus by *Elodea densa*. *Hydrobiologia* 111, 43–48. <https://doi.org/10.1007/BF00007379>.
- Gelman, A., Carlin, J.B., Stern, H.S., Dunson, D.B., Vehtari, A., Rubin, D.B., 2013. Bayesian Data Analysis, 3rd ed. Chapman and Hall/CRC, Boca Raton, FL. <https://doi.org/https://doi.org/10.1201/b16018>.
- Gilks, W.R., Richardson, S., Spiegelhalter, D., 1998. Markov Chain Monte Carlo in Practice. Chapman and Hall/CRC, Boca Raton, FL.
- Government of Canada, 2017. Great Lakes water quality agreement: areas of concern [WWW Document]. Gov. Canada. URL <https://www.canada.ca/en/environment-climate-change/services/great-lakes-protection/canada-united-states-water-quality-agreement/areas-concern.html>.
- Government of Canada, 2016. Water sources: wetlands [WWW Document]. Gov. Canada. URL <https://www.canada.ca/en/environment-climate-change/services/water-overview/sources/wetlands.html>.
- Granéli, W., Solander, D., 1988. Influence of aquatic macrophytes on phosphorus cycling in lakes. *Hydrobiologia* 170, 245–266. <https://doi.org/10.1007/BF00024908>.
- Gudimov, A., Ramin, M., Labencki, T., Wellen, C., Shelar, M., Shimoda, Y., Boyd, D., Arhonditsis, G.B., 2011. Predicting the response of Hamilton Harbour to the nutrient loading reductions: A modeling analysis of the “ecological unknowns” *J. Great Lakes Res.* 37, 494–506.
- Hamilton Conservation Authority, 2018. Watershed Report Card 2018. Ancaster, ON.
- Hamilton Harbour RAP Technical Team, 2010. Contaminant Loadings and Concentrations to Hamilton Harbour: 2003–2007 update. Burlington, ON.
- Hamilton Harbour Water Quality Technical Team, 2007. Hamilton Harbour RAP Water Quality Goals and Targets Review - Part 1: Response to the City of Hamilton's Proposed Wastewater System Upgrades. Burlington, ON.
- Harrison, K.T., Theysmeijer, T., 2014. Turtles of Royal Botanical Gardens Site Specific Recovery Plan. Hamilton, Ontario.
- Herb, W.R., Stefan, H.G., 2003. Integral growth of submersed macrophytes in varying light regimes. *Ecol. Modell.* 168, 77–100. [https://doi.org/10.1016/S0304-3800\(03\)00206-0](https://doi.org/10.1016/S0304-3800(03)00206-0).
- Hughes, K.D., de Solla, S.R., Weseloh, D.V.C., Martin, P.A., 2016. Long-term trends in legacy contaminants in aquatic wildlife in the Hamilton Harbour Area of Concern. *Aquat. Ecosyst. Heal. Manag.* 19, 171–180. <https://doi.org/10.1080/14634988.2016.1150113>.
- Ibelings, B.W., Portielje, R., Lammens, E.H.R.R., Noordhuis, R., van den Berg, M.S., Joosse, W., Meijer, M.L., 2007. Resilience of alternative stable states during the recovery of shallow lakes from eutrophication: Lake Veluwe as a case study. *Ecosystems* 10, 4–16. <https://doi.org/10.1007/s10021-006-9009-4>.
- Infrastructure Canada, 2013. Major Wastewater Infrastructure Improvements Help Clean Up Hamilton Harbour [WWW Document]. Infrastruct. Canada <http://www.infrastructure.gc.ca/media/news-newspages/2013/20130626hamilton-eng.html>.
- Isely, P., Isely, E.S., Hause, C., Steinman, A.D., 2018. A socioeconomic analysis of habitat restoration in the Muskegon Lake area of concern. *J. Great Lakes Res.* 44, 330–339.
- Janse, J.H., van Dam, A.A., Hes, E.M.A., de Klein, J.J.M., Finlayson, C.M., Janssen, A.B.G., van Wijk, D., Moolij, W.M., Verhoeven, J.T.A., 2019. Towards a global model for wetlands ecosystem services. *Curr Opin Environ Sustain* 36, 11–19. <https://doi.org/10.1016/j.cosust.2018.09.002>.
- Kim, D.-K., Javed, A., Yang, C., Arhonditsis, G.B., 2018. Development of a mechanistic eutrophication model for wetland management: Sensitivity analysis of the interplay among phytoplankton, macrophytes, and sediment nutrient release. *Ecol. Inform.* 48, 198–214. <https://doi.org/10.1016/j.ecoinf.2018.09.010>.
- Kim, D.-K., Peller, T., Gozum, Z., Theysmeijer, T., Long, T., Boyd, D., Watson, S., Rao, Y.R., Arhonditsis, G.B., 2016. Modelling phosphorus dynamics in Cootes Paradise marsh: Uncertainty assessment and implications for eutrophication management. *Aquat. Ecosyst. Heal. Manag.* 19, 368–381. <https://doi.org/10.1080/14634988.2016.1255097>.
- Kim, D.-K., Yang, C., Parsons, C.T., Bowman, J., Theysmeijer, T., Arhonditsis, G.B., 2019. Examination of the existence of alternative ecological states in a eutrophic wetland using mechanistic modelling. [Submitted Manuscript].
- Leisti, K.E., Theysmeijer, T., Doka, S.E., Court, A., 2016. Aquatic vegetation trends from 1992 to 2012 in Hamilton Harbour and Cootes Paradise. Lake Ontario. *Aquat. Ecosyst. Health Manag.* 19, 219–229. <https://doi.org/10.1080/14634988.2015.1129257>.
- Long, T., Wellen, C., Arhonditsis, G., Boyd, D., 2014. Evaluation of stormwater and snowmelt inputs, land use and seasonality on nutrient dynamics in the watersheds of Hamilton Harbour, Ontario, Canada. *J. Great Lakes Res.* 40, 964–979. <https://doi.org/https://doi.org/10.1016/j.jglr.2014.07.001>.

- [org/10.1016/j.jglr.2014.09.017](https://doi.org/10.1016/j.jglr.2014.09.017).
- Long, T., Weller, C., Arhonditsis, G., Boyd, D., Mohamed, M., O'Connor, K., 2015. Estimation of tributary total phosphorus loads to Hamilton Harbour, Ontario, Canada, using a series of regression equations. *J. Great Lakes Res.* 41, 780–793. <https://doi.org/10.1016/j.jglr.2015.04.001>.
- Loughheed, V.L., Chow-Fraser, P., 1998. Factors that regulate the zooplankton community structure of a turbid, hypereutrophic Great Lakes wetland. *Can. J. Fish. Aquat. Sci.* 55, 150–161.
- Loughheed, V.L., Theysmeyer, T., Smith, T., Chow-Fraser, P., 2004. Carp exclusion, food-web interactions, and the restoration of Cootes Paradise Marsh. *J. Great Lakes Res.* 30, 44–57. [https://doi.org/10.1016/S0380-1330\(04\)70328-7](https://doi.org/10.1016/S0380-1330(04)70328-7).
- Madgwick, F.J., 1999. Restoring nutrient-enriched shallow lakes: Integration of theory and practice in the Norfolk Broads, U.K. *Hydrobiologia* 408 (409), 1–12. https://doi.org/10.1007/978-94-017-2986-4_1.
- Markovic, S., Liang, A., Watson, S.B., Depew, D., Zastepa, A., Surana, P., Vandenberg-Byllaardt, J., Arhonditsis, G., Dittrich, M., 2019. Reduction of industrial iron pollution promotes phosphorus internal loading in eutrophic Hamilton Harbour, Lake Ontario, Canada. *Environ. Pollut.* 252, 697–705.
- Mao, D., Cherkaier, K.A., 2009. Impacts of land-use change on hydrologic responses in the Great Lakes region. *J. Hydrol.* 374, 71–82. <https://doi.org/10.1016/j.jhydrol.2009.06.016>.
- Mataya, K., Court, A., and J.E. Bowman. 2017. Project Paradise Season Summary 2016. RBG Report No. 2017-9. Royal Botanical Gardens. Hamilton, Ontario.
- Mayer, T., Rosa, F., Charlton, M., 2005. Effect of sediment geochemistry on the nutrient release rates in Cootes Paradise Marsh, Ontario, Canada. *Aquat. Ecosyst. Health Manag.* 8, 133–145. <https://doi.org/10.1080/14634980590954986>.
- Millennium Ecosystem Assessment, 2005. Ecosystems and Human Well-Being: Wetlands and Water Synthesis. Washington, DC. <https://doi.org/10.1017/CBO9781107415324.004>.
- Moss, B., Stansfield, J., Irvine, K., Perrow, M., Phillips, G., 1996. Progressive Restoration of a Shallow Lake: A 12-Year Experiment in Isolation, Sediment Removal and Biomanipulation. *J. Appl. Ecol.* 33, 71–86.
- Parsons, C.T., Rezanezhad, F., O'Connell, D.W., Van Cappellen, P., 2017. Sediment phosphorus speciation and mobility under dynamic redox conditions. *Biogeosciences* 14, 3585–3602. <https://doi.org/10.5194/bg-14-3585-2017>.
- Pascual, U., Muradian, R., Brander, L., Gómez-Baggethun, E., Martín-López, B., Verma, M., Armsworth, P., Christie, M., Cornelissen, H., Eppink, F., Farley, J., Loomis, J., Pearson, L., Perrings, C., Polasky, S., 2010. The Economics of Valuing Ecosystem Services and Biodiversity, in: Kumar, P. (Ed.) *The Economics of Ecosystems and Biodiversity Ecological and Economic Foundations*. Earthscan, London. <https://doi.org/10.4324/9781849775489>.
- Prescott, K.L., Tsanis, I.K., 1997. Mass balance modelling and wetland restoration. *Ecol. Eng.* 9, 1–18. [https://doi.org/10.1016/S0925-8574\(97\)00015-3](https://doi.org/10.1016/S0925-8574(97)00015-3).
- Ramin, M., Stremilov, S., Labencki, T., Gudimov, A., Boyd, D., Arhonditsis, G.B., 2011. Integration of numerical modeling and Bayesian analysis for setting water quality criteria in Hamilton Harbour, Ontario, Canada. *Environ. Model. Softw.* 26, 337–353. <https://doi.org/10.1016/j.envsoft.2010.08.006>.
- Reddick, D., Theysmeyer, T., 2012. 20 Year Trends in Water Quality Cootes: Cootes Paradise and Grindstone Creek Marsh. Hamilton, Ontario.
- Scheffer, M., Carpenter, S., Foley, J.A., Folke, C., Walker, B., 2001. Catastrophic shifts in ecosystems. *Nature* 413, 591–596. <https://doi.org/10.1038/35098000>.
- Smith, T., Lundholm, J., Simser, L., 2001. Wetland Vegetation Monitoring in Cootes Paradise: Measuring the Response to a Fishway/Carp Barrier. *Ecol. Restor.* 19, 145–154.
- Spiegelhalter, D., Thomas, A., Best, N., Lunn, D., 2003. WinBUGS User Manual.
- Suding, K.N., Gross, K.L., Houseman, G.R., 2004. Alternative states and positive feedbacks in restoration ecology. *Trends Ecol. Evol.* 19, 46–53. <https://doi.org/10.1016/j.tree.2003.10.005>.
- Tammeorg, O., Horppila, J., Laugaste, R., Haldna, M., Niemistö, J., 2015. Importance of diffusion and resuspension for phosphorus cycling during the growing season in large, shallow Lake Peipsi. *Hydrobiologia* 760, 133–144. <https://doi.org/10.1007/s10750-015-2319-9>.
- Theysmeyer, T., 2011. Project Paradise Planning to 2015. Royal Botanical Gardens, Hamilton, Ontario.
- Theysmeyer, T., J. Bowman. 2017. Western Desjardins Canal and West Pond Conditions Summary Report. Natural Lands Department. Internal Report No. 2017-1. Royal Botanical Gardens. Hamilton, Ontario.
- Theysmeyer, T., J. Bowman, A. Court, and S. Richer. 2016. Wetlands Conservation Plan 2016–2021. Natural Lands Department. Internal Report No. 2016-1. Royal Botanical Gardens. Hamilton, Ontario.
- Theysmeyer, T., Galbraith, D., 2007. Biedermann Packaging Fire: Effects on Cootes Paradise marsh. Hamilton, Ontario.
- Theysmeyer, T., Reich, B., Bowman, J., 2009. Water Quality Characterization of the Main Tributaries of the Garden's Property: Spencer Creek, Chedoke Creek, Borer's Creek, Grindstone Creek 2008/09. Hamilton, Ontario.
- Thomassen, S., Chow-Fraser, P., 2012. Detecting changes in ecosystem quality following long-term restoration efforts in Cootes Paradise Marsh. *Ecol. Indic.* 13, 82–92. <https://doi.org/10.1016/j.ecolind.2011.04.036>.
- Trudeau, M.P., Richardson, M., 2016. Empirical assessment of effects of urbanization on event flow hydrology in watersheds of Canada's Great Lakes-St Lawrence basin. *J. Hydrol.* 541, 1456–1474. <https://doi.org/10.1016/j.jhydrol.2016.08.051>.
- Trolle, D., Nielsen, A., Andersen, H.E., Thodsen, H., Olesen, J.E., Børgesen, C.D., Refsgaard, J.C., Sonnenborg, T.O., Karlsson, I.B., Christensen, J.P., Markager, S., Jeppesen, E., 2019. Effects of changes in land use and climate on aquatic ecosystems: Coupling of models and decomposition of uncertainties. *Sci Total Environ.* 657, 627–633. <https://doi.org/10.1016/j.scitotenv.2018.12.055>.
- Troy, A., Bagstad, K., 2013. Estimation of Ecosystem Service Values for Southern Ontario. Ottawa, ON.
- Troy, A., Wilson, M.A., 2006. Mapping ecosystem services: Practical challenges and opportunities in linking GIS and value transfer. *Ecol. Econ.* 60, 435–449. <https://doi.org/10.1016/j.ecolecon.2006.04.007>.
- Twilley, R.R., Ejding, G., Romare, P., Kemp, W.M., 2019. A Comparative Study of Decomposition, Oxygen Consumption and Nutrient Release for Selected Aquatic Plants Occurring in an Estuarine Environment. *Oikos* 47, 190–198.
- Wilcox, D.A., Whillans, T.H., 1999. Techniques for restoration of disturbed coastal wetlands of the Great Lakes. *Wetlands* 19, 835–857.

**PREDICTING THE LIKELIHOOD OF A DESIRABLE
ECOLOGICAL REGIME SHIFT: A CASE STUDY IN COOTES
PARADISE MARSH, LAKE ONTARIO, ONTARIO, CANADA**

[SUPPORTING INFORMATION]

**Cindy Yang¹, Dong-Kyun Kim¹, Jennifer Bowman², Tys Theësmeÿer²,
George B. Arhonditsis^{1*}**

**¹Ecological Modelling Laboratory, Department of Physical &
Environmental Sciences, University of Toronto, Toronto, Ontario,
Canada, M1C 1A4**

² Royal Botanical Gardens, Burlington, Ontario L7T 4H4, Canada

* Corresponding author

E-mail: georgea@utsc.utoronto.ca, Tel.: +1 416 208 4858; Fax: +1 416 287 7279.

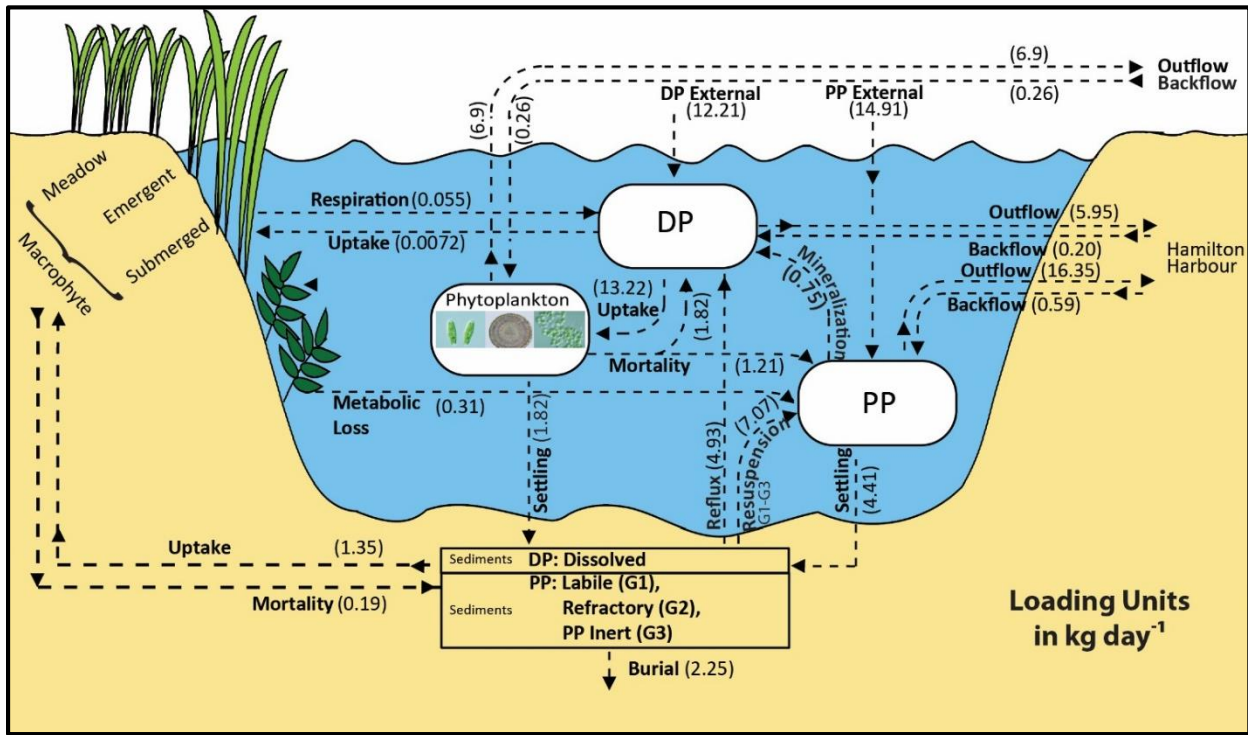


Figure S1: Average daily phosphorus (P) fluxes derived from the mechanistic model during the growing season (May–October) from 1996 to 2012. Fluxes for different functional groups were summed within macrophytes, phytoplankton and sediment compartments. Details on the model fit against chlorophyll *a* and TP measured concentrations, parameter values assigned during the model calibration, and the characterization of the simulated biogeochemical processes in Cootes Paradise marsh are presented in Kim et al. (2019)¹.

¹ Kim D-K., Yang C., Parsons C.T., Bowman J., Theysmeijer T., Arhonditsis, G.B., 2019. Examination of the existence of alternative ecological states in a eutrophic wetland using mechanistic modelling. Submitted Manuscript.

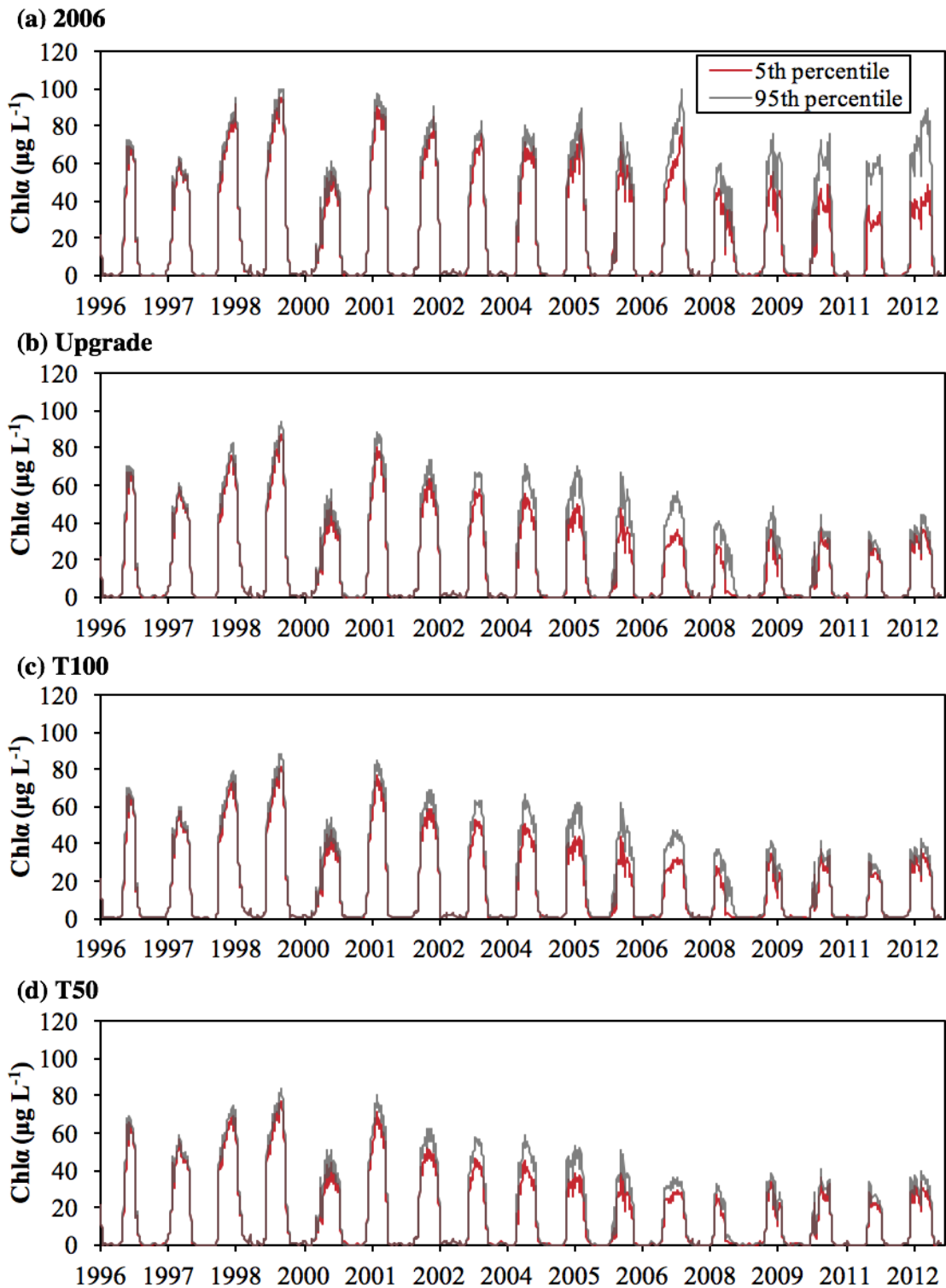
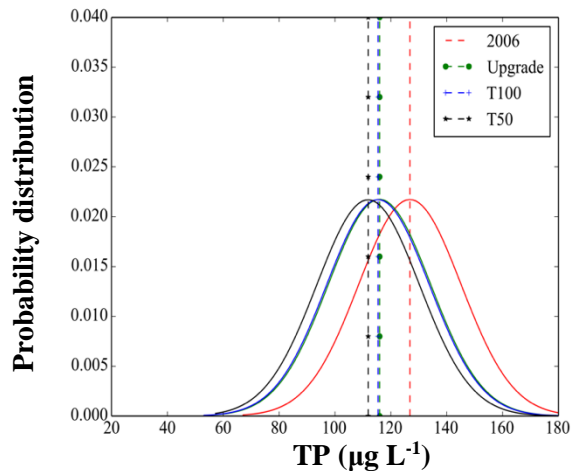
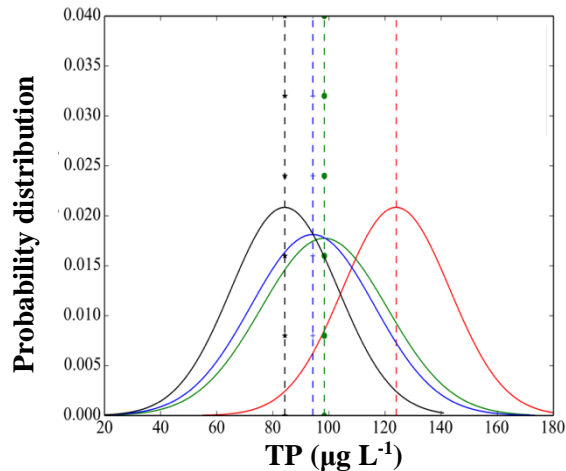


Figure S2: 90% uncertainty bounds for Chl α concentrations predicted by the mechanistic model based on different Dundas WWTP loading scenarios: (a) 2006, (b) Upgrade, (c) T100, and (d) T50. The scenario 2006 represent the year with the worst loading conditions between 2005-2016; The Upgrade scenario is based on the 2013 conditions when the Dundas WWTP upgrades were completed; T100 examines the potential improvements from an average TP effluent concentrations of 100 $\mu\text{g L}^{-1}$; T50 examines the potential improvements from an average TP effluent concentrations of 50 $\mu\text{g L}^{-1}$.

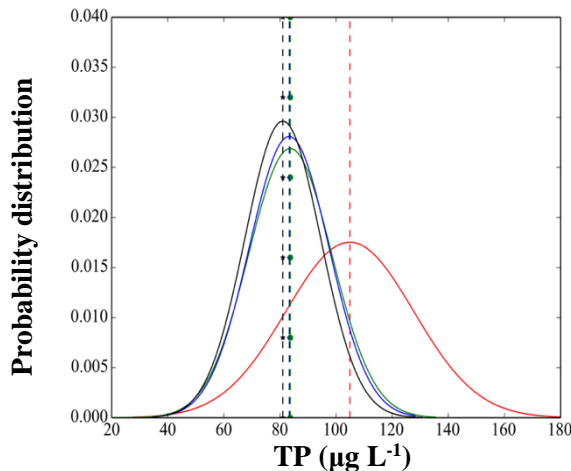
(a) Submerged macrophyte P sequestration: 1.5



(b) Submerged macrophyte P sequestration: 3.0



(c) Submerged macrophyte P sequestration: 3.5



(d) Submerged macrophyte P sequestration: 4.5

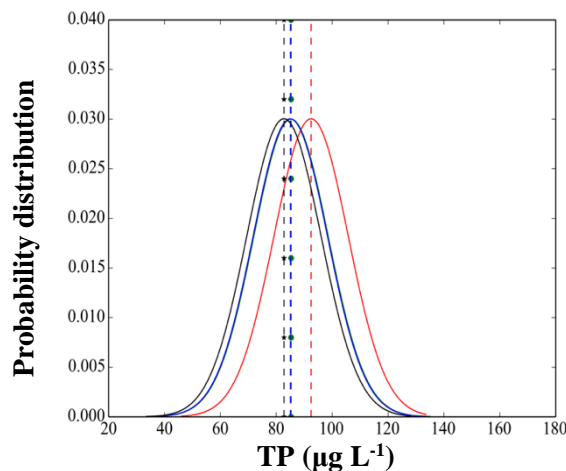


Figure S3: (a-d) Predictive distributions of seasonal TP concentrations averaged over the 2008-2012 period in response to different loading scenarios from the Dundas WWTP and varying degrees of P sequestration from the submerged aquatic vegetation. The latter process was emulated by the combined variation of respiration ($0.0135\text{-}0.0165 \text{ day}^{-1}$) and mortality ($0.0432\text{-}0.0528 \text{ day}^{-1}$) of submerged macrophytes, and P quota in macrophyte biomass. Numbers on the top of each panel represent the multipliers used to increase the strength of P sequestration relative to the reference conditions ($0.0025 \text{ g P g DW}^{-1}$) assigned by [Kim et al. \(2019\)](#), e.g., 1.5, 3.0, 3.5, and 4.5 reflect P quotas in plant tissues equal to 0.00375 , 0.0075 , 0.00875 , and $0.01125 \text{ g P g DW}^{-1}$. The uncertainty of TP concentrations stems from the variability associated with the tributary loading, which was accommodated by inducing $\pm 15\%$ perturbations of the present conditions.

Table S1: Posterior estimates of the stochastic nodes of the feedforward statistical modelling framework for Cootes Paradise marsh.

Parameter	Model segment <i>i</i>	Notation	Definition	Unit	Mean	SD	2.5%	97.5%	Odds*
Baseline Intercepts	1	β_{WP0}	Background level of TP_{WP}	$\ln(\mu\text{g } TP_i \text{ L}^{-1})$	5.11	1.71	1.76	8.49	
	2	β_{CW0}	Background level of TP_{CW}		8.10	0.48	7.16	9.01	
	3	β_{CC0}	Background level of TP_{CC}		3.70	0.34	3.04	4.37	
	4	γ_{CC0}	Background level of $Chla_{CC}$		-0.35	0.69	-1.75	1.05	
Model Errors	1	σ_{WP}	Residual variability for TP_{WP} not explained by model	$\ln(\mu\text{g } TP_i \text{ L}^{-1})$	0.36	0.02	0.33	0.40	
	2	σ_{CW}	Residual variability for TP_{CW} not explained by model		0.34	0.02	0.31	0.37	
	3	σ_{CC}	Residual variability for TP_{CC} not explained by model		0.41	0.02	0.37	0.46	
	4	τ_{CC}	Residual variability for $Chla_{CC}$ not explained by model		0.07	0.04	0.02	0.17	
Slopes	1	$\beta_{WP1^{**}}$	Change in TP_{WP} for a unit change in TP_{Dundas}	$\frac{\ln(\mu\text{g } TP_{WP} \text{ L}^{-1})}{\ln(\mu\text{g } TP_{Dundas} \text{ L}^{-1})}$	0.34	0.05	0.23	0.45	>99.9%
	1	β_{WP2}	Change in TP_{WP} for a unit change in Q_{Dundas}	$\frac{\ln(\mu\text{g } TP_{WP} \text{ L}^{-1})}{\ln(\text{m}^3 \text{ day}^{-1})}$	-0.18	0.17	-0.52	0.15	85.3%
	2	$\beta_{CW1^{**}}$	Change in TP_{CW} for a unit change in TP_{WP}	$\frac{\ln(\mu\text{g } TP_{CW} \text{ L}^{-1})}{\ln(\mu\text{g } TP_{WP} \text{ L}^{-1})}$	0.12	0.07	-0.01	0.25	96.1%
	2	$\beta_{CW2^{**}}$	Change in TP_{CW} for a unit change in TP_{SC}	$\frac{\ln(\mu\text{g } TP_{CW} \text{ L}^{-1})}{\ln(\mu\text{g } TP_{SC} \text{ L}^{-1})}$	0.25	0.04	0.17	0.32	>99.9%

2	β_{CW3}	Change in TP_{CW} for a unit change in Q_{SC}	$\frac{\ln (\mu\text{g } TP_{CW} \text{ L}^{-1})}{\ln (\text{m}^3 \text{ day}^{-1})}$	-0.41	0.02	-0.45	-0.37	>99.9%
3	β_{CC1**}	Change in TP_{CC} for a unit change in TP_{CW}	$\frac{\ln (\mu\text{g } TP_{CC} \text{ L}^{-1})}{\ln (\mu\text{g } TP_{CW} \text{ L}^{-1})}$	0.24	0.07	0.11	0.37	>99.9%
4	γ_{CC1}	Change in $Chla_{CC}$ for a unit change in TP_{CC}	$\frac{\ln (\mu\text{g } Chla_{CC} \text{ L}^{-1})}{\ln (\mu\text{g } TP_{CC} \text{ L}^{-1})}$	0.60	0.18	0.23	0.96	>99.9%
4	γ_{CC2}	Change in $Chla_{CC}$ for a unit change in TP_{WD}	$\frac{\ln (\mu\text{g } Chla_{CC} \text{ L}^{-1})}{\ln (\mu\text{g } TP_{WD} \text{ L}^{-1})}$	0.16	0.21	-0.28	0.55	78.0%

*Odds of the slope regression coefficients being positive/negative is the probability mass above/below zero. The magnitude of the odds were classified such that >90%, 70-90%, and 50-70% probability of a positive/negative slope regression coefficient were indicative of a strong, medium, and weak relationship.

**Unitless parameters. The selected presentation of their units is intended to facilitate their interpretation.

Table S2: Year-specific intercepts of the TP and Chla models developed for the central area of Cootes Paradise marsh. To facilitate parameter identification, these among year-effect terms are constrained to have a zero sum, and their units are in [$\ln(\mu\text{g TP L}^{-1})$] and [$\ln(\mu\text{g Chla L}^{-1})$], respectively.

Year	$\beta_{CCY} (TP_{Centre})$					$\gamma_{CCY} (Chla_{Centre})$				
	Mean	SD	2.5%	Median	97.5%	Mean	SD	2.5%	Median	97.5%
1994	0.16	0.11	-0.05	0.15	0.38	0.04	0.09	-0.09	0.03	0.25
1995	0.08	0.10	-0.13	0.08	0.28	0.00	0.07	-0.16	0.00	0.14
1996	0.13	0.11	-0.09	0.12	0.36	0.02	0.08	-0.12	0.01	0.21
1997	-0.46	0.14	-0.72	-0.46	-0.18	-0.05	0.09	-0.29	-0.03	0.08
1998	-0.02	0.10	-0.21	-0.02	0.18	0.00	0.08	-0.16	0.00	0.16
1999	0.15	0.13	-0.09	0.14	0.41	0.01	0.08	-0.14	0.01	0.17
2000	0.03	0.11	-0.19	0.03	0.25	0.01	0.08	-0.14	0.01	0.19
2001	0.19	0.11	-0.01	0.19	0.40	0.01	0.08	-0.14	0.01	0.18
2002	-0.05	0.10	-0.25	-0.05	0.16	0.02	0.08	-0.13	0.02	0.21
2003	0.08	0.10	-0.12	0.08	0.28	0.04	0.08	-0.10	0.03	0.24
2004	-0.04	0.10	-0.23	-0.03	0.15	-0.02	0.07	-0.20	-0.01	0.11
2005	0.03	0.10	-0.16	0.03	0.22	0.00	0.08	-0.15	0.00	0.16
2006	-0.06	0.10	-0.26	-0.06	0.14	-0.01	0.08	-0.17	0.00	0.15
2007	0.19	0.10	-0.01	0.18	0.39	0.01	0.07	-0.14	0.00	0.17
2008	-0.15	0.11	-0.38	-0.15	0.06	0.00	0.07	-0.16	0.00	0.15
2009	-0.05	0.10	-0.24	-0.04	0.15	0.01	0.07	-0.14	0.01	0.16
2010	0.00	0.10	-0.19	0.00	0.20	-0.01	0.08	-0.17	0.00	0.14
2011	-0.01	0.10	-0.21	-0.01	0.18	0.00	0.07	-0.16	0.00	0.16
2012	0.02	0.10	-0.17	0.02	0.22	0.00	0.08	-0.17	0.00	0.15
2013	-0.23	0.12	-0.47	-0.23	0.02	-0.08	0.21	-0.49	-0.09	0.35

Table S3: Month-specific intercepts of the *TP* and *Chla* models developed for the central area of Cootes Paradise marsh. To facilitate parameter identification, these within year-effect terms are constrained to have a zero sum, and their units are in [$\ln(\mu\text{g TP L}^{-1})$] and [$\ln(\mu\text{g Chla L}^{-1})$], respectively.

Year	$\beta_{CCM} (TP_{Centre})$					$\gamma_{CCM} (Chla_{Centre})$					
	Mean	SD	2.5%	Median	Mean	SD	2.5%	SD	Mean	SD	
May	-0.13	0.12	-0.40	-0.12	0.10		-0.19	0.08	-0.34	-0.19	-0.04
June	-0.25	0.10	-0.46	-0.25	-0.04		0.01	0.05	-0.10	0.01	0.12
July	0.12	0.10	-0.06	0.12	0.31		0.12	0.06	0.01	0.12	0.23
August	0.20	0.10	0.00	0.20	0.39		0.07	0.06	-0.04	0.07	0.18
September	0.06	0.11	-0.17	0.06	0.27		-0.01	0.06	-0.13	0.00	0.12